1968 Annual Progress Report
of
Palaeogeophysics Research in Japan

1 9 6 8

Osaka

1. Magnetic and Crystallographic Investigations of Small Spherules Found in Deep-sea Sediments

Kazuo Kobayashi and Kazuhiro Kitazawa

Ocean Research Institute, University of Tokyo

Abstract

Thermomagnetic and X-ray analysis provided some information on the material identification of small black spherules and pinkish translucent ones found in red clay collected at the western equatorial Pacific. It was suggested that the black spherules are possibly magnetite. The translucent ones have not yet been identified. No definite evidence was found regarding the origin of the two types of spherules.

1. Samples

During the cruise KH67-5 of the R/V Hakuho-maru two types of small spherules were found in red clay collected at two stations (st39: $16^{\circ}41'$N, $176^{\circ}21'$W, and st40: $17^{\circ}17'$N, $176^{\circ}18'$W) in the western equatorial Pacific (Fig.1). Sizes of the spherules range between 0.1 mm and 1.0 mm in diameter. However, as the spherules were obtained after they were screened by sieves with roughly 0.1 mm meshes, it may be possible that smaller ones were lost, if any existed.

One type of spherule has black color and smooth metal-like surface. The other is translucent and colors pale pink for the reflected light. The former is strongly magnetic and can easily be extracted with a small handy permanent magnet.

2. Magnetic properties

One whole piece of black spherule was set in a magnetic balance. Magnetization was measured in magnetic fields amounting to 12.4 Koe.

Absolute intensity of magnetization was calibrated using a paramagnetic salt the susceptibility of which was known and the intensity of saturation magnetization J_s was determined according to the $^1/_H$ law of approach to saturation. The intensity of the saturation magnetization at room temperature is listed in Table 1 with two samples (1A and 1B). Two averaged value of J_s is then 86.5 emu/gr which is nearly equal to that of stoichiometric magnetite (Fe_3O_4, J_s=92 emu/gr).

Magnetization was then measured at higher temperatures. The sample was heated in vacuum of about 10^{-3} mmHg of air. Maximum temperature of heating was stepwisely increased but intensity of magnetization was reversible in respect to temperature (Fig.2). This result indicates that the black spherule is quite free from any chemical or physicochemical change at high temperature in vacuum. There exist no polymorphic transitions accompanied with magnetic change such as observed in some Ni-Fe alloys at around 500°C.

The Curie temperature determined from this thermomagnetic curve is about 570°C which is also consistent with that of Fe_3O_4. The curve shows no other magnetic phases with different Curie temperature. The black spherule seems, therefore, likely to be homogeneous in composition.

Fig. 2 shows the a-c demagnetization curves of saturation isothermal remanence at room temperature which indicate the spectrum of remanent coercive force of black spherules. The averaged remanent coercive force is roughly 100 oe which may be moderate if the demagnetizing effect of spherical shape is considered.

The translucent spherules are very weak in magnetism. A high-sensitive magnetic balance (sensitivity 10^{-6} emu) could detect no deflection when a sample of 0.903 mg was set in a field of 5 Koe.

3. X-ray Analysis

Debye-Scherrer method was used to determine the crystallographic structure of these spherules. The X-ray diffractometer for powder specimens was useless because of the small quantity of samples. In Debye-Scherrer photography the Fe target of X-ray was used with no filter. The diffraction pattern of a black spherule shown in Table 2-a can be indexed on a basis of a cubic spinel structure with the lattice parameter a=8.33Å which is again similar to that of Fe_3O_4.

The diffraction lines of the translucent spherules (Table 2-b) are, on the contrary, very difficult to be identified by the ASTM index cards. No corresponding mineral name or chemical formula has been found, although it seems likely that they are admixture of silicates with no free magnetic ions such as ferrous, ferric or manganese ions.

4. Discussion and geophysical significance

The present experimental results seem to indicate that the black magnetic spherules in deep-sea sediment consist of homogeneous magnetite (Fe_3O_4). The diffraction pattern may not reveal the inner structure of the spherules if their nucleus have different composition. However, if the nucleus is composed of a ferromagnetic material another Curie temperature must be detected in the thermomagnetic curves. Only the exception is the case where the Curie point of the nucleus is coincident with 570°C. Such a case is very limited, for instance, in 55 atomic % Ni-45 atomic % Fe and 75 atomic % Ni-25 atomic % Fe, if the nucleus is Ni-Fe alloy. The problem is more complex if the nucleus is non-ferromagnetic. Finally more detailed investigation such as by the microprobe analyzer will clarify this problem.

Similar magnetic spherules as well as silicate ones in deep-sea sediments have been reported by several authors (e.g. Pettersson and

Fredriksson 1958) since Murray discovered them and described as cosmic spherules in a book "The Depths of the Ocean" (Murray and Hjort, republished 1965).

One of the most important evidences of the cosmic origin of spherules was their chemical composition identical with that of iron meteorites. Castaing and Fredriksson (1958) showed the shell structure of some spherules by the microanalyzer technique. It is uncertain whether the present samples belong to a particular case without a metallic nucleus or they are completely of a different origin.

The present study provided no data on the relative abundance of the magnetic spherules in deep-sea sediment. If the abundance is relatively large in wide areas, the spherules can not be disregarded as one of the magnetic constituents of deep-sea sediments which are now very important in paleomagnetism. As their remanent coercive force is relatively high, natural remanent magnetization of the sediment can be at least partly carried by these spherules. The natural remanence may be purely of depositional in such a case and assure the paleomagnetic reliability except a problem of the inclination errors.

Table 1

Characteristic numerical values of typical deep-sea spherules

	1A	1B	2
Diameter	0.6 mm	0.5 mm	0.9 mm
Weight	0.407 mg	0.335 mg	0.903 mg
J_s (20°C)	85.7 emu/gr	87.3 emu/gr	0
T_c	-----	570°C	-----
a	8.33 Å	-----	unidentified
color	black	black	pale-pink translucent

Table 2a

Debye-Scherrer pattern of a black spherule (1A)

2θ	Intensity	Index
125.05	S	(553,731)
119.53	vw	(642)
98.50	w	(533)
81.75	s	(440)
74.30	w	(333,511)
45.33	s	(311)
42.40	vw	
38.38	vw	(220)

Table 2b

Debye-Scherrer pattern of a translucent spherule

2	d	Intensity
104.00	1.228	w
91.35	1.353	vw
89.20	1.379	
82.70	1.465	w
73.78	1.612	vw
71.90	1.649	
69.25	1.703	vw
66.73	1.761	vw
38.78	2.914	s
36.58	3.083	vs
35.73	3.158	vs
23.28	4.794	s

vs; very strong, s; strong, w;weak, vw; very weak, not denoted; trace

Figure Captions

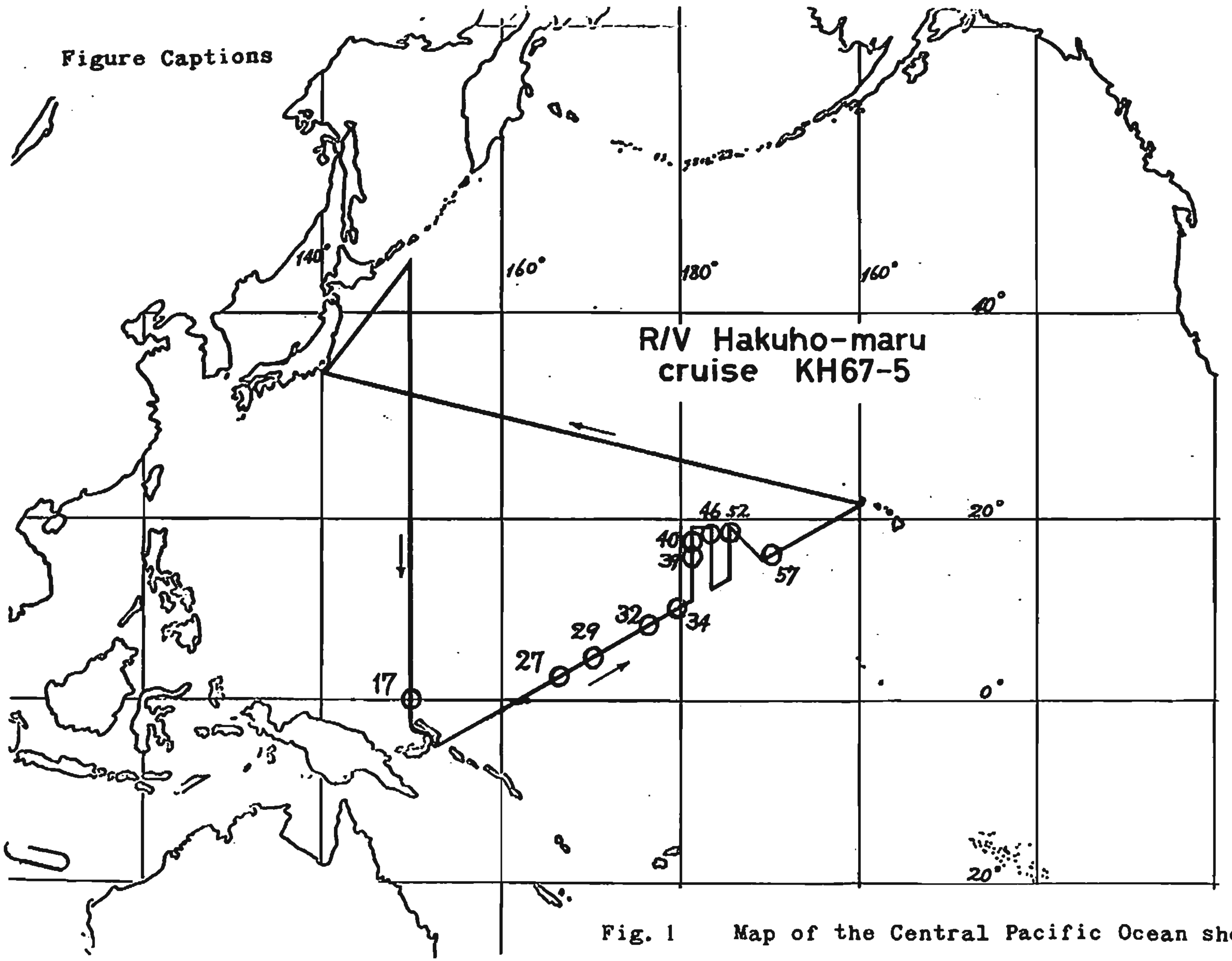

Fig. 1 Map of the Central Pacific Ocean showing the ship's track of the Cruise KH 67-5 by the R/V Hakuho-maru. Numerical figures indicate the station No.

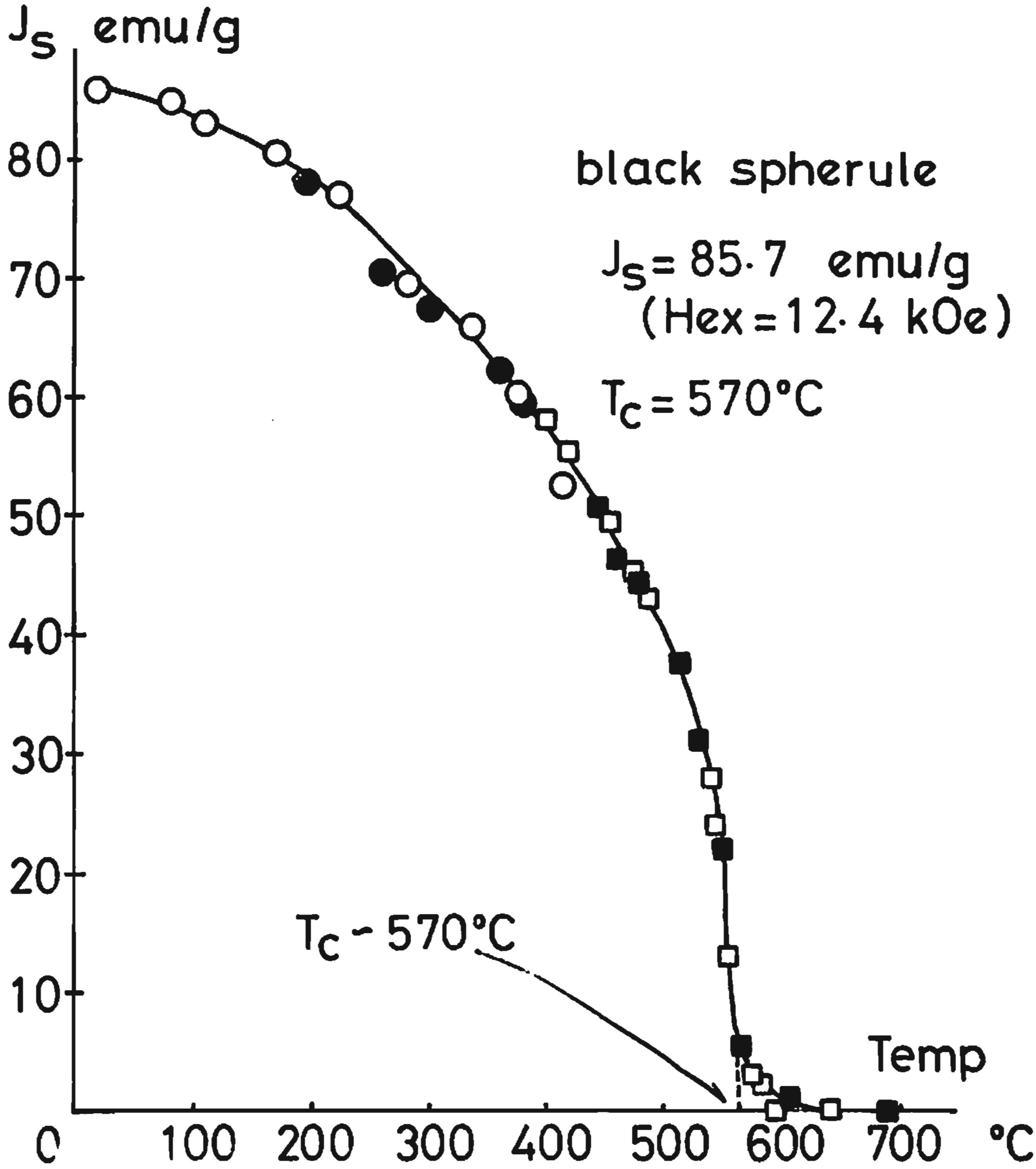

Fig. 2 Thermomagnetic curve of a black deep-sea spherule.

--○-- 1st heating

--●-- 1st cooling

--□-- 2nd heating

--■-- 2nd cooling

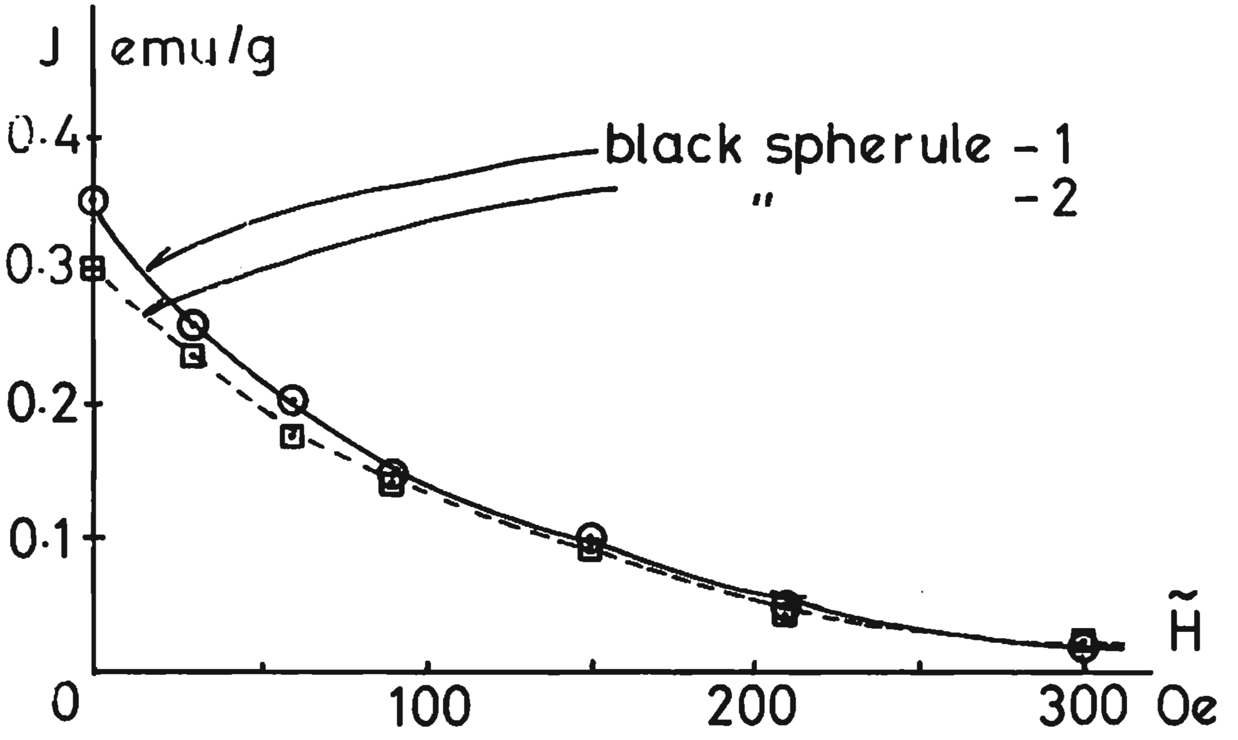

Fig. 3 A.c.-demagnetization curves of saturation isothermal remanence of black spherules.

2. Fission Track Registration as an Advanced Technique for Dating Terrestrial Materials

Susumu Nishimura

Department of Geological Sciences, University of Osaka Prefecture

Recent development in fission track technique has provided geologists and archaeologists with a new promising tool with which to date various igneous rocks, or many baked relics. [1,2]

In this short report it describe one of our actual dating experiments by showing the result of several Plio-Pleistocene volcanic tuffs belonging to Osaka Group. The tuffs contain following minerals suitable for the dating; anthophillite, apatite, hornblende and zircon respectively.

The fission track age, T (y), can be represented by the following equation

$$T=\frac{1}{\lambda}\ln\left(1+\frac{\lambda}{\lambda_f}\frac{\rho_s}{\rho_i}\frac{\phi\sigma}{\eta}\frac{R_i}{R_s}\right)\cdots\cdots\cdots\cdots\cdots (1)$$

where, ρ_s is spontaneous track density, (cm^{-2}), ρ_i is induced track density by bombardment with thermal neutron, (cm^{-2}), λ is total decay constant for uranium, (y^{-1}), λ_f is fission decay constant for ^{238}U, (y^{-1}), ϕ is thermal neutron dose, (cm^{-2}), σ is thermal cross section for fission ^{235}U, (cm^{-2}), η is isotope ratio $^{235}U/^{238}U$, and R_s and R_i are the mean value of the etchable length of the fragments produced by a spontaneous fission and that produced by the induced fission, (cm).

If T were smaller than 10^9 y, eq. 1 can be written as

$$T=6.12\times10^{-8}\ \phi\ \frac{\rho_s}{\rho_i}\ \frac{R_i}{R_s}\cdots\cdots\cdots\cdots\cdots\cdots (2)$$

It is suggested clearly in Fig. 1 and Table 1, that there exist in the actual analysis of the fission track determination several questions still remain unsolved. For example, a question arises as to whether the age thus obtained along above-mentioned calculation shows much older age when the mineral we employed in the experiment formed originally in the volcanic cones. Another question remains as to whether determination of the neutron flux used in this experiment is sufficiently reasonable as well as reliable. Although we used quite steady flux density of the thermal neutron beam to irradiate our sample, the time was so short that fluctuation of the flux should be taken into account. For this purpose we employed a comparator standard with which the actual flux exposure was determined. [3] Usually, our minerals were so small in diameter, that a number of same minerals were observed in order to count the number of spontaneous fission.

This method of dating terrestrial materials is unexpectedly accurate as well as satisfactory. The method is also far less expensive for us who could eliminate the purchase and maintenance of the mass-spectrometer to obtain ^{40}K-^{40}Ar ratio.

References

1) Fleischer, R. L., Price, P. M., Symes, E. M. and Miller, D. S., (1964), Science, 143, 349.

2) Fleischer, R. L., Price, P. M. and Walker, R. M., (1965), Jour. Geophys. Res., 70, 1497.

3) Nishimura, S., (1968), Archaeo. Sci., 1, 46, (in Japanese).

Table 1. Fission track age of some tuffs of Osaka Group

Sample	ρ_s (cm ^{2})	ρ_i (cm ^{2})	ϕ (cm ^{2})	Fission track age (m.y.)	Note
Anthophillite	4.32×10^{3}	3.02×10^{5}	0.48×10^{15}	0.42	Kasuri tuff
	3.28×10^{3}	2.68×10^{5}	0.48×10^{15}	0.36	
	6.01×10^{3}	$5.04\times1C^{5}$	0.48×10^{15}	0.35	
				mean 0.38 ± 0.03	
Apatite	2.06×10^{4}	4.11×10^{5}	1.26×10^{15}	0.37 ± 0.04	
Hornblende	7.25×10^{3}	5.47×10^{5}	1.11×10^{15}	0.90	Azuki tuff
	6.50×10^{3}	5.16×10^{5}	1.11×10^{15}	0.85	
	6.61×10^{3}	5.16×10^{5}	1.11×10^{15}	0.87	
				mean 0.87 ± 0.07	
Zircon	5.6×10^{6}	1.5×10^{8}	0.46×10^{15}	1.1 ± 0.1	Komyoike tuff
Hornblende	2.3×10^{3}	8.2×10^{4}	1.50×10^{15}	2.3 ± 0.2	Shimakumayama tuff
Zircon	1.7×10^{7}	2.0×10^{8}	0.46×10^{15}	2.4 ± 0.3	
Zircon	1.85×10^{7}	1.8×10^{8}	0.46×10^{15}	2.9 ± 0.4	Sagami tuff

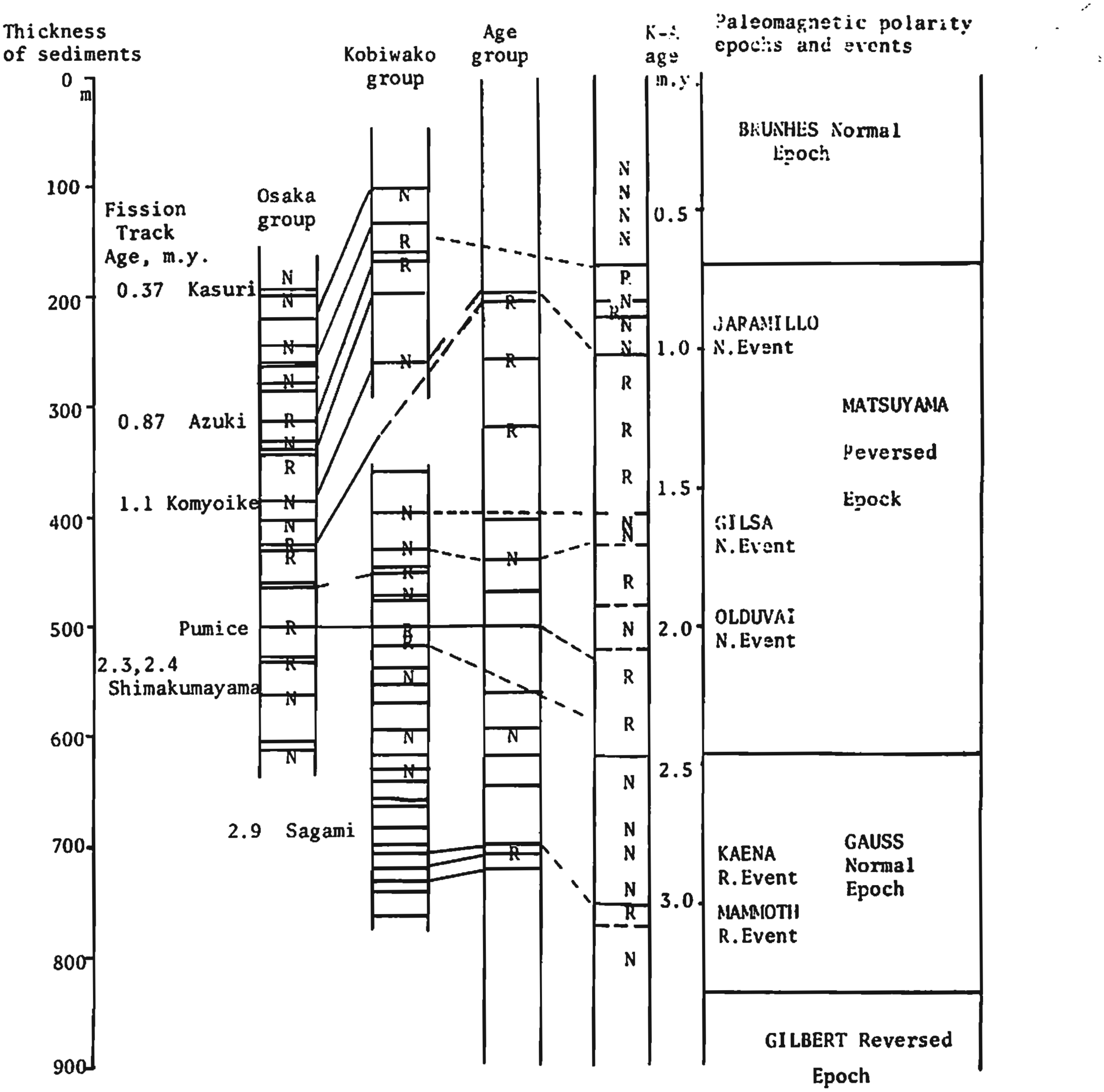

Thickness of sediments
0 m
100
200
300
400
500
600
700
800
900
Fission Track Age, m.y.
0.37 Kasuri
0.87 Azuki
1.1 Komyoike
Pumice
2.3,2.4 Shimakumayama
2.9 Sagami
Osaka group
Kobiwako group
Age group
K-A age m.y.
0.5
1.0
1.5
2.0
2.5
3.0
Paleomagnetic polarity epochs and events
BRUNHES Normal Epoch
JARAMILLO N.Event
MATSUYAMA Reversed Epoch
GILSA N.Event
OLDUVAI N.Event
KAENA R.Event
MAMMOTH R.Event
GAUSS Normal Epoch
GILBERT Reversed Epoch

3. Fission Track Dating of Archaeological Materials from Japan

Masao Suzuki and Naotune Watanabe

Department of Anthropology, The University of Tokyo,

Tokyo, Japan

As the nuclear fission takes place in uranium atoms contained in a mineral, nuclear fragments which split out of the nucleus cause a kind of damage along their tracks in the mineral. This sort of tracks is called the fission track which was first observed by an electron microscope (Silk and Barnes, 1959) and made visible under an optical microscope by chemical etching of minerals (Price and Walker, 1962).

Fission track dating method depends on the facts that U^{238} atoms in a mineral are subject to the apontaneous fission which occurs at a constant disintegration rate, and that fission tracks once produced in a mineral disappear if the mineral is heated above a relevant critical temperature (Fleischer and Price, 1963). So, it is reasonably assumed that the number of fission tracks in a mineral is proportional to the lapse of time after the mineral was last heated above the critical temperature and the total number of U^{238} atoms contained in the mineral. The latter is reduced from the number of fission tracks of U^{235} atoms which are induced by attacking the mineral with a known dose of thermal neutrons using the natural abundance of U^{238} and U^{235} atoms.

If the fission track density per 1 cm^2 of fracture surface of a glass is determined with regard to the spontaneous fission of U^{238} ρ_s , and the induced fission of U^{235} ρ_i after the irradiation of the material with a dose of thermal neutrons φ, the lapse of time T either after the glass was produced or after it was last heated above the critical temperature is approximately given by

$$\rho_s/\rho_i = [\exp(\lambda_D T) - 1] \; (\lambda_f/\lambda_D \varphi\sigma I)$$

where λ_f is the spontaneous fission decay constant of U^{238} (6.85×10^{-17} yr^{-1}: Fleischer and Price, 1964), λ_D is the total decay constant of U^{238} (1.54×10^{-10} yr^{-1}), σ is the cross section for thermal neutron-induced fission of U^{235} (582×10^{-24} cm^2), and I is the natural abundance ratio of U^{235} to U^{238} (7.26×10^{-3}).

Then T is simply given by (Fleischer, Price, Walker and Leakey, 1965a)

$$T = 6.12 \times 10^{-8} \varphi(\rho_s/\rho_i)$$

The method has rather rarely been applied to materials of anthropological and archaeological interest: obsidian fragments from the formation at Olduvai Gorge where bones of Zinjanthropus had been found was dated two million years in good agreement with the potassium-argon date (Fleischer et al., 1965a), glass vessels of high uranium contents of the nineteenth and twentyth century (Brill, Fleischer, Price and Walker, 1964) and an obsidian mesolithic knife blade from Elementeita in East Africa (Fleischer, Price, Walker and Leakey, 1965b) were also dated by this method.

The authors applied the method to archaeological glass materials from Japan and the present paper deals with the results obtained so far.

<u>Materials</u> (1) Obsidian spearhead from Tosamporo. A broken piece of obsidian spearhead, 4.3 cm in length, was found imbedded in the body of a pottery vase from dwelling pit No.25 at Tosamporo in Nemuro city, Hokkaido. The pottery vase is fibre-tempered, pointed-bottomed and decorated with a kind of impressed pattern, which are all characteristic of the earliest Jomon pottery in Hokkaido (Iwasaki and Maeda, 1966). For experiment an about 0.2 g piece was cut from a broken end of the spearhead by a water-cooled diamond-charged saw.

(2) Obsidian arrowhead and obsidian flake from Onnemoto. These two obsidian specimens, 3.5 cm and 2.5 cm long respectively, were collected from dwelling pit No.2 at Onnemoto in Nemuro city, Hokkaido. It is a dwelling pit destroyed by fire and both specimens are wilted in shape

indicating that they were heated to a high temperature. The associated pottery is of the Okhotsk type.

(3) Glaze of a bowl from Seto. A fragment of bowl was collected from a ceramic kiln named Tsubaki-gama of the Middle age in Seto city, central Honshu. On the surface of the potsherd dripped glaze formed a dark brown coloured glass layer. A part on which the glaze measured more than 1 mm in thickness was cut out for assay.

Method Specimens were abraded to expose a fresh inner portion of glass, which was polished and then etched by 48% hydrofluoric acid solution for 15 - 25 seconds at the room temperature. As the reagent attacks the damaged part of glass along fission tracks more rapidly than the general part of glass, cone-shaped pits are formed at positions where fission tracks were cut by the polished surface. Spontaneous fission track density per 1 cm^2 was determined by counting the number of etched pits observed in the field of microscope the area of which was measured with a lattice micrometer. As the etched pits were observed so sporadically that the procedures of polishing, etching and counting was repeatedly applied to the same surface of glass to count a sufficient number of etched tracks. The same piece of specimen was then irradiated with thermal neutrons and the induced fission track density was determined through similar procedures as mentioned above with regard to spontaneous fission tracks.

The track fading temperature, that is the critical temperature at which fission tracks fade out, was determined by such a procedure that a sample which was irradiated with thermal neutrons was heated step by step at an increasing temperature and everytime it was surveyed if fission tracks were observable or not.

Results Conditions of experiment and results obtained are given in Table 1. The error of fission track dates refers to the standard deviation of counting track pits.

As to the fission track date of the obsidian spearhead from Tosamporo, two radiocarbon dates are available for comparison 3240: ±160 years (I-1506) and 3900 ± 120 years B.P.(N-266). These radiocarbon dates were obtained from charcoal collected at the dwelling pit No.30 which was 30 m distant from the dwelling pit No. 25. As the pottery associated with those dwelling pits are mainly of the same type, it may be assumed that the dwelling pits were used almost contemporaneously and the radiocarbon dates indicate the approximate age of the obsidian spearhead. It has been said, however, that these radiocarbon dates might be too young to be taken as those of the earliest Jomon period in Hokkaido. The reason is that they are exceptionally young among six radiocarbon dates so far obtained from the relevant period in Hokkaido and also they are comparable to or much younger than six radiocarbon dates from the early and middle Jomon periods in Hokkaido which are all older than 3800 years. In this respect it may be suggestive that the obsidian spearhead yielded the fission track date which was nearly 1000 or 2000 years older than the relevant radiocarbon dates.

As the result of annealing experiment, it revealed that the track fading temperature of the specimen was 350 - 400°C. This means that the fission tracks once existed in the specimen disappeared at the time when the pottery vase was made because the Jomon pottery in general must have been fired at a temperature above 550°C (Eto, 1963). Accordingly, it is out of question that spontaneous fission tracks observed in the specimen were formed after the pottery vase had been manufactured.

An obsidian arrowhead and an obsidian flake from Onnemoto were, as mentioned above, wilted in shape. To make a rough measurement of wilting temperature of these obsidian materials, a piece of obsidian flake was heated at increasing temperature in an electric furnace. As the result, it began to wilt at a temperature between 850 and 900°C suggesting that the obsidian arrowhead and flake were heated to such a high temperature when the dwelling pit caught a fire. Fission track dates obtained from the two specimens fall within the range of their standard deviation. The flake specimen gave a rather large value of standard deviation because it contained many small bubbles which made the counting of track pits difficult. Similar small bubbles were observed in some obsidian flakes which were heated above 850°C in an electric furnace. While charcoal collected from the dwelling pit No. 2 which yielded the specimens has not been assayed, there are six radiocarbon dates which are associated with the Okhotsk type pottery. They are 990 ± 140 years (GaK-190), 1180 ± 100 years (TK-9), 1230 ± 100 years (TK-2), 1240 ± 90 years (TK-54), 1310 ± 120 years (GaK-191) and 1420 ± 170 years B.P.(GaK-189), and the fission track dates of specimens from Onnemoto correspond to the younger part of the range of these radiocarbon dates. Accordingly to the historical division of age, they fall in the early Heian era.

In respect to the ceramic kilns Tsubaki-gama in Seto, no radiocarbon dates are available yet. However, from archaeological and historical point of view, it has been said that the kilns were used in the period from the Kamakura to the Muromachi era ranging from the thirteenth to sixteenth century. The fission track date obtained from the glaze corresponds to the middle of the Muromachi era. The track fading temperature of this specimen was as low as 170 - 230°C. In this respect, cutting and polishing procedures were carefully applied to the specimen so as to keep the temperature of specimen as low as possible.

Besides the fission track dates shown in Table 1, approximate values of the uranium content of specimens were also obtained from the induced fission track density which was determined by counting etched tracks on a polycarbonate sheet placed on the specimen at the time of thermal neutron irradiation. The values for the spearhead from Tosamporo, the arrowhead and the obsidian flake from Onnemoto, and the glaze of a bowl from Seto were 3.2, 3.1, 3.1 and 3.3 ppm by weight respectively. It is obvious that to date archaeological materials of such a young age as millennia or centuries, the uranium content of materials must be correspondingly high. If materials which meet this requirement are available, the fission track dates obtained from these materials may provide a reliable chronological background for studies in archaeology and anthropology.

The authors wish to express their gratitudes to Dr. M. Shima for valuable advices, to Dr. M. Hattori and Mr. K. Kato for kind help in attacking samples with thermal neutrons, and to Profs. I. Yawata and N. Kokubu, and Mr. T. Iwasaki for submitting materials.

References

Brill, R. H., R. L. Fleischer, P. B. Price, and R. M. Walker (1964), The Fission-track Dating of Man-made Glasses: Preliminary Results, J. Glass Studies, 6, 151-155.

Eto, M. (1963), Firing Temperature of Jomon Pottery, J. Anthrop. Soc. Nippon, 121, 23-51.

Fleischer, R. L., and P. B. Price (1963), Charged Particle Tracks in Glass, J. Appl. Phys., 34, 2903-2904.

Fleischer, R. L., and P. B. Price (1964), Techniques for Geological Dating of Minerals by Chemical Etching of Fission Fragment Tracks, Geochim. Cosmochim. Acta, 28, 1705-1714.

Fleischer, R. L., P. B. Price, R. N. Walker, and L. S. B. Leakey (1965a), Fission Track Dating of a Mesolithic Knife, Nature, 205, 1138.

Fleischer, R. L., P. B. Price, R. M. Walker, and L. S. B. Leakey (1965b), Fission-track Dating of Bed I, Olduvai Gorge, Science, 148, 72-74.

Iwasaki, T., and U. Maeda (1966), Tosamporo Site. in: Prehistoric Sites in Nemuro City, Hokkaido, published by the Board of Education of Nemuro City, 109-218.

Price, P. B., and R. M. Walker (1962), Chemical Etching of Charged-Particle Tracks in Solids, J. Appl. Phys., 33, 3407-3412.

Silk, E. C. H., and R. S. Barnes (1959), Examination of Fission Fragment Tracks with an Electron Microscope, Phil. Mag., 4, 970-972.

Table 1

Specimen		Etching Conditions 48%HF-23°C	Dose of Thermal Neutron Flux φ	Induced Fission Track Pits ρ_i	Spontaneous Fission Track Pits ρ_s		Age of Specimen T	Track Fading Temperature
		sec.	n.u.t.	Density per cm²	Total count -total area cm²	Density per cm²	ys. B.P.	°C
Tosamporo	Obsidian Spearhead	15	1.8 $\times 10^{15}$	1.00 $\times 10^{5}$	175 - 37.9	4.62	5080±400	350-400
Onnemoto	Obsidian arrowhead	15	0.3 $\times 10^{15}$	0.16 $\times 10^{5}$	44 - 47.6	0.92	1060±160	350-400
	Obsidian flake	15	0.3 $\times 10^{15}$	0.16 $\times 10^{5}$	7 - 7.0	1.00	1150±440	350-400
Seto	Glaze on a bowl	25	1.8 $\times 10^{15}$	0.75 $\times 10^{5}$	25 - 71.0	0.33	520±110	170-230

4. Archaeo-Aurora and Geomagnetic Secular Variation in Historic Time

Mitsuo Keimatsu

College of Liberal Arts, Kanazawa University

Naoshi Fukushima and Takesi Nagata

Geophysics Research Laboratory, University of Tokyo

In order to trace the secular variation of the geomagnetic field in historic time, the documents of ancient aurorae can be utilized. In China, Korea and Japan, there are a number of valuable records, which can be reasonably supposed to describe the event of auroral appearance. After a comparison of these descriptions with those in Europe, the archaeo-secular variation in the geomagnetic field can be inferred.

A comparison of the auroral appearance on the same day in the Occident and Orient suggests that the geomagnetic dipole axis might have been inclined towards China around 11 - 12th Centuries A.D. This conclusion seems to be in accordance with the result obtained by Kawai et al. (1965), though our analysis is still of insufficient accuracy to test the wobbling motion of the geomagnetic field in historic time as suggested by Kawai and Hirooka (1967). An outline of our study is already published (Keimatsu, Fukushima and Nagata, 1967, 1968).

It is worthwhile to extend the study of ancient aurorae in more detail in order to contribute to clarifying the secular geomagnetic variation in historic time. One of the authors (Keimatsu, 1965) picked up a number of descriptions of aurorae or auroral-like phenomena in the Chinese, Korean and Japanese literatures, from 7 B.C. to 10 A.D. for the present purpose. He is preparing an English text for the ancient aurorae in the Oriental region, and the first report the Chinese document in B.C. is now in press (Keimatsu, 1969).

References

Kawai, N. and K. Hirooka (1967), Wobbling motion of the geomagnetic dipole field in historic time during these 2000 years, J. Geomag. Geoelectr., 19, 217-227.

Kawai, N., K. Hirooka and S. Sasajima (1965), Counterclockwise rotation of the geomagnetic dipole axis revealed in the world-wide archaeo-secular variations, Proc. Japan Acad., 41, 398-403.

Keimatsu, M. (1965), Documentary catalogue of northern lights observed in China, Korea and Japan from 7 B.C. to 10 A.D. (Preprint, college of Liberal Arts, Kanazawa University.

Keimatsu, M. (1969), A chronology of aurorae and sunspots extending over China, Korea and Japan, Part I, submitted to J. Geomag. Geoelectr.

Keimatsu, M., N. Fukushima and T. Nagata (1967), Archaeo-aurora and geomagnetic secular variation in historic time, 1967 Annual Progress Report of Palaeo-geophysics Research in Japan; (1968), J. Geomag. Geoelectr., 20, 45-50.

5. Separation of the Earth's Magnetic Field into the Drifting and the Standing Parts

Takesi Yukutake

Earthquake Research Institute, University of Tokyo

The non-dipole part of the earth's magnetic field has long been believed to undergo a considerably rapid time variation, and the whole part originates from the same source within the earth's core. However, recent investigation of the non-dipole field over the past several centuries has revealed the existence of two types of non-dipole regional anomalies, the anomalies standing at the same locality and those drifting westwards (Yukutake and Tachinaka, 1968a). It has been confirmed that most of the conspicuous anomalies are standing ones and that only a few exhibit drifting. Some of the standing anomalies change their intensity very rapidly, and the others remain constant. In the 18th century, the non-dipole field in the northern hemisphere seems to have undergone a drastic change. A strong positive anomaly in the Central Pacific almost disappeared and the Mongolian anomaly started to increase.

Although many of the predominant non-dipole anomalies have remained nearly at the same place during the last several hundred years, the whole distribution of the geomagnetic secular variation has been confirmed to be drifting on a global scale (Yukutake and Tachinaka, 1968b). The scalar potentials of the geomagnetic secular variation along parallel circles were expanded in Fourier series and the drift rates of the individual harmonic components were examined (Yukutake, 1968). The mean rates over the various parallel circles were calculated for each harmonic number m and listed in Table 1.

Let us assume that the Gauss-Schmidt coefficients of the geomagnetic field g_n^m and h_n^m can be represented by the standing part and the drifting one as follows,

$$g_n^m(t) = F_n^m \cos\varphi_n^m + K_n^m \cos mv_n^m(t - \tau_n^m)$$

$$-h_n^m(t) = F_n^m \sin\varphi_n^m + K_n^m \sin mv_n^m(t - \tau_n^m),$$

where F_n^m and τ_n^m are the amplitude and the phase angle of the standing component, and K_n^m, φ_n^m represent the amplitude of the drifting component and its phase measured in the unit of time. v_n^m is the drift velocity measured in 0.01°/year and t is time with the origin at 1800 A.D. defined by

$$t = (T - 1800)/100$$

where T is the epoch in the year A.D.

Since the geomagnetic secular variation likely gives a better approximation for the velocity of the drifting field than the main field does, the velocity model listed in Table 1 was adopted as v_n^m to separate the field into two types.

Applying a sort of least squares method to eleven sets of the Gauss-Schmidt coefficients covering the period from 1600 to 1965 A.D., F_n^m, φ_n^m, K_n^m and τ_n^m were obtained as in Table 2 (Yukutake and Tachinaka, 1968c). It should be noted that, as far as the harmonic terms up to n=m=3, drifting terms (K_n^m) dominate over standing terms (F_n^m) except for n=3, m=2. For n=2, m=2, the drifting term is several times larger than the standing one.

From the results, the standing parts of the non-dipole field, were synthesized and shown in Fig. 1 for the vertical component. Similarly the drifting parts are shown in Fig. 1. The main features of the standing anomalies are very similar to those of the non-dipole field itself. This is probably due to the fact that the most predominating anomalies such as the Mongolian and the North American anomalies are the standing ones. As may be expected from the preponderance of the lower harmonics, the distribution of the drifting field is much simpler than the standing field.

From the two types of field separated above, we can calculate the earth's field for any epoch. It has been confirmed that thus synthesized field from the drifting and standing component can well approximate the observed field. An example is shown in Fig. 2. Distributions of the vertical component along parallel circles of 40°N and the equator are shown for various epochs. Solid lines denote the observed field and the broken lines the synthetic field from the two type fields. The calculated field well approximates the general property of the observed one and its secular variation.

No systematic behaviour of the differences between the observed field and the calculated from the present steady model of two type fields is noticed for the last several hundred years. This indicates that both the drifting and the standing fields are very stable and steady. Another noteworthy property of the secular variation is non-existence of interference between the two type fields. It seems to suggest that they are of separate origins. From consideration of free decay time, some of the standing field are likely to have their sources within the solid part of the earth.

References

T. Yukutake (1968), The drift velocity of the geomagnetic secular variation, J. Geomag. Geoelect., 20, in press.

T. Yukutake and H. Tachinaka (1968a), The non-dipole part of the earth's magnetic field, Bull. Earthq. Res. Inst., 46, 1027-1074.

T. Yukutake and H. Tachinaka (1968b), The westward drift of the geomagnetic secular variation, Bull. Earthq. Res. Inst., 46, 1075-1102.

T. Yukutake and H. Tachinaka (1968c), Separation of the earth's magnetic field into the drifting and the standing parts, Bull. Earthq. Res. Inst., 46, in press.

Figure Captions

Fig. 1. Standing field and drifting field of the non-dipole vertical component.

Fig. 2a. Distribution of the vertical component along 40°N parallel and its variation with time. Solid lines denote the observed distributions, broken lines calculated ones.

Fig. 2b. Distribution of the vertical component along the equator and its variation with time. Solid lines denote the observed distributions, broken lines calculated ones.

Table 1 Velocity models obtained from the secular variation.

Dispersive velocities for Fourier components when the potential along parallels are expanded in Fourier series

$v_n^1 = 0.166\ ^{\circ}/\mathrm{yr}.$	
$v_n^2 \quad 0.339\ ^{\circ}/\mathrm{yr}.$	
$v_n^3 = 0.269\ ^{\circ}/\mathrm{yr}.$	
$v_n^4 = 0.189\ ^{\circ}/\mathrm{yr}.$	
$v_n^n = 0.3\ ^{\circ}/\mathrm{yr}.$	for $m \geqq 5$

Table 2 The standing and the drifting parts of the earth's magnetic field.

F_n^m; amplitude of the standing component.

φ_n^m; phase angle of the standing component.

K_n^m; amplitude of the drifting component.

τ_n^m; phase of the drifting component measured in time unit.

n	m	F_n^m	φ_n^m	K_n^m	τ_n^m
1	1	3503 γ	-78.4°	3896 γ	9.70
2	1	1571	112.9	3570	1.31
2	2	399	139.8	1879	1.68
3	1	1607	-124.7	1907	-5.47
3	2	1076	-7.9	225	1.14
3	3	342	-39.8	540	1.36
4	1	920	25.9	556	7.26
4	2	638	34.1	121	2.42
4	3	231	118.4	252	-1.33
4	4	224	68.4	161	1.71
5	1	479	27.9	179	8.73
5	2	291	-4.0	54	-1.69
5	3	54	167.0	63	0.71
5	4	113	127.3	35	-0.65
5	5	101	-60.1	81	0.64
6	1	58	45.8	48	4.83
6	2	49	-148.5	67	2.22
6	3	154	172.1	45	-1.09
6	4	20	170.9	5	0.24
6	5	104	-95.3	55	1.03
6	6	40	-176.8	34	0.57

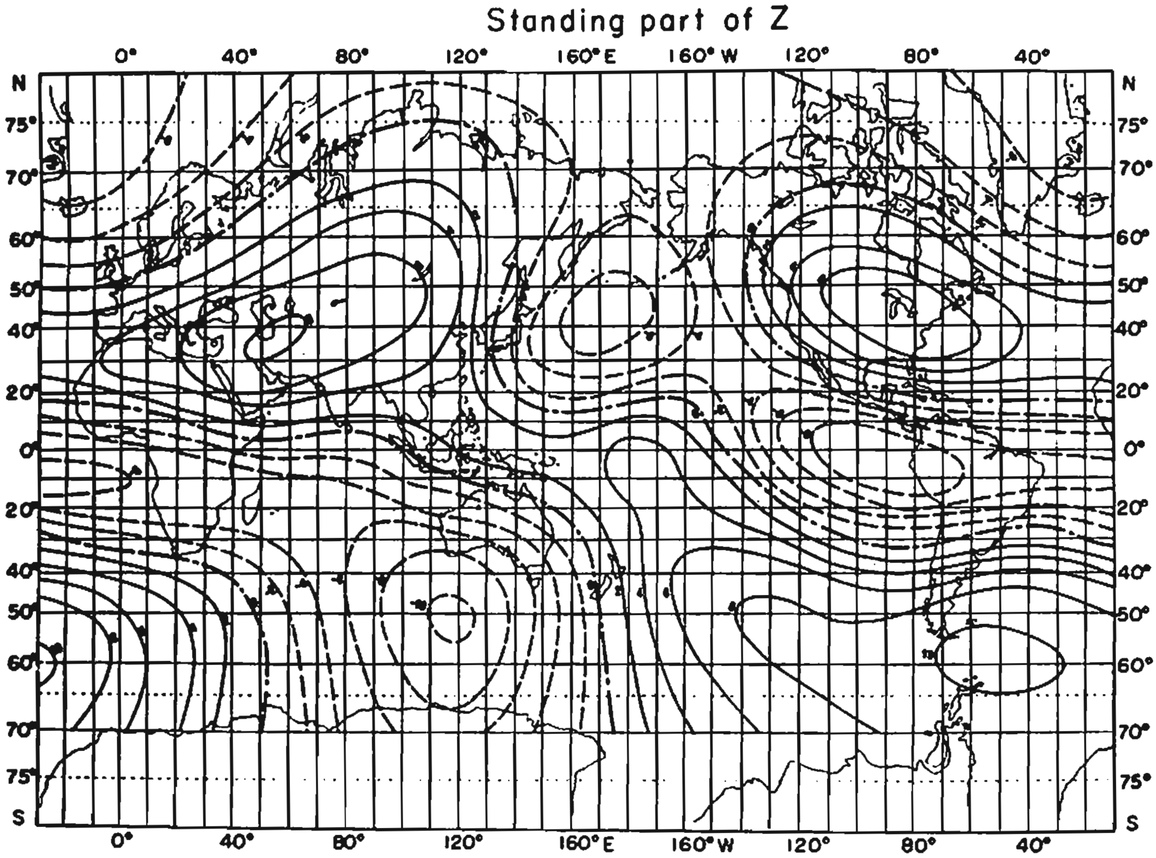
Standing part of Z
0°
40°
80°
120°
160°E
160°W
120°
80°
40°
N
75°
70°
60°
50°
40°
20°
0°
20°
40°
50°
60°
70°
75°
S

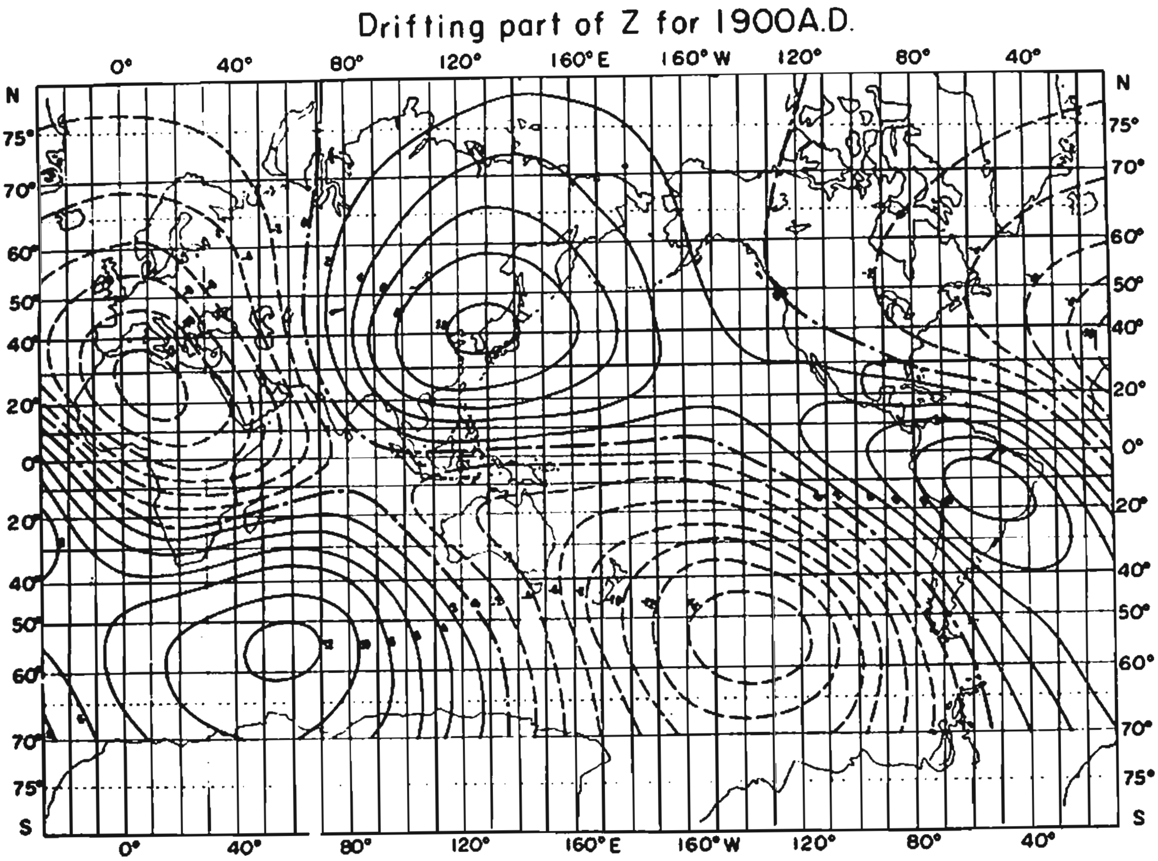
Drifting part of Z for 1900A.D.
0°
40°
80°
120°
160°E
160°W
120°
80°
40°
N
75°
70°
60°
50°
40°
20°
0°
20°
40°
50°
60°
70°
75°
S

Fig. 1

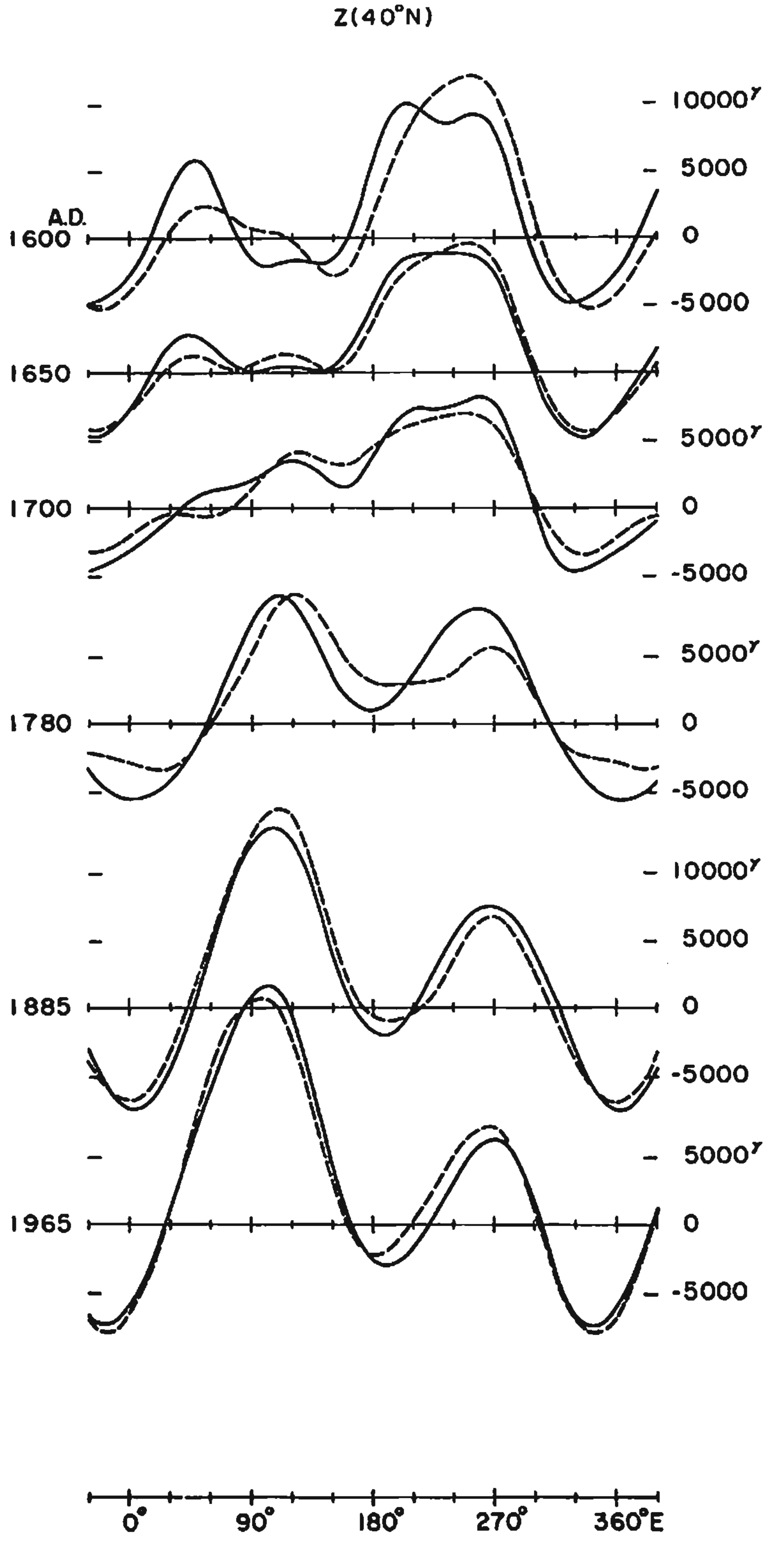
Z(40°N)
A.D.
1600
1650
1700
1780
1885
1965
10000γ
5000
0
-5000
5000γ
0
-5000
5000γ
0
-5000
10000γ
5000
0
-5000
5000γ
0
-5000
0°
90°
180°
270°
360°E

Fig. 2

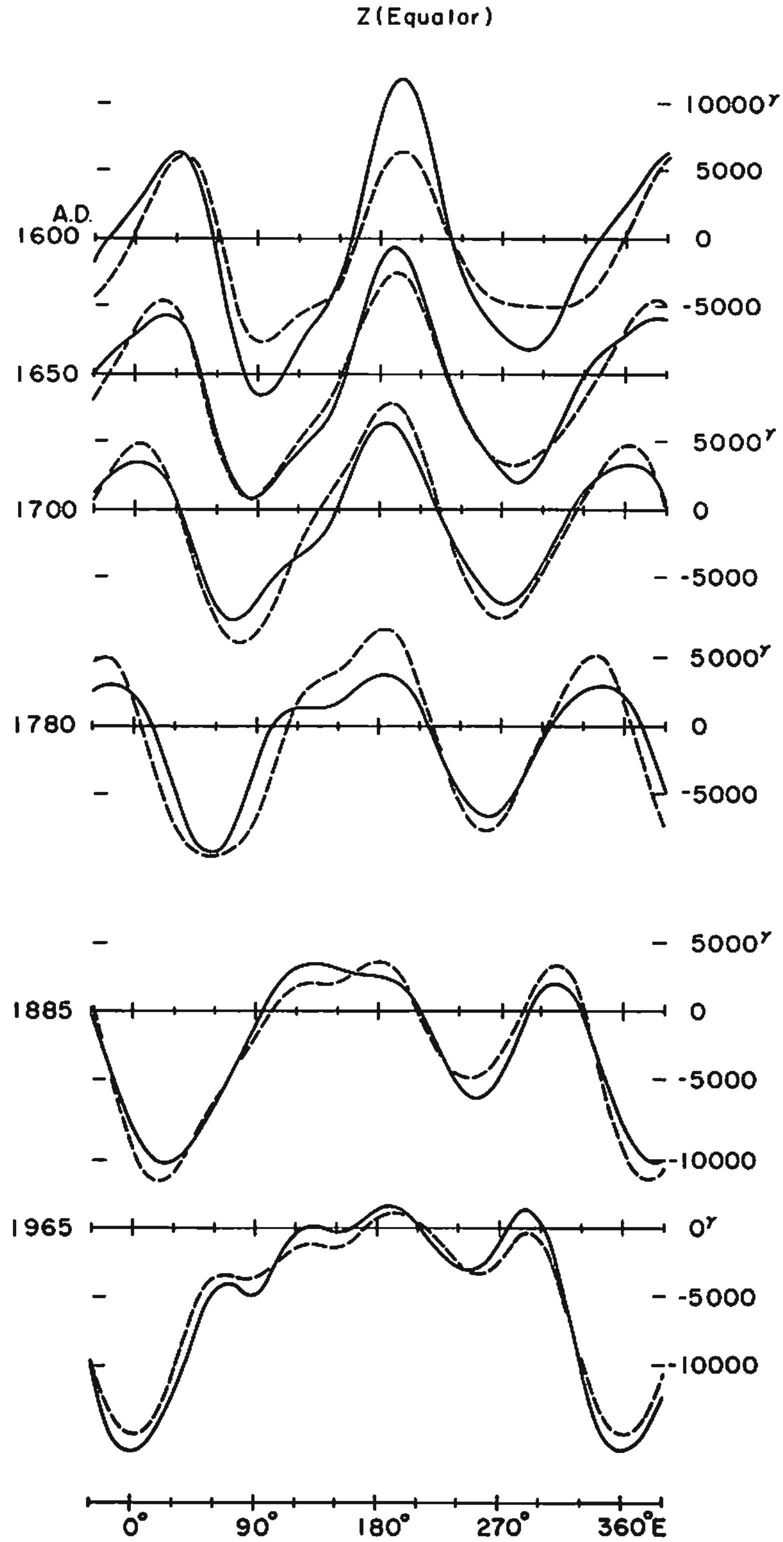
Z (Equator)
A.D.
1600
1650
1700
1780
1885
1965
10000γ
5000
0
-5000
5000γ
0
-5000
5000γ
0
-5000
5000γ
0
-5000
-10000
0γ
-5000
-10000
0°
90°
180°
270°
360°E

Fig. 3

6. Intensity of the Earth's Magnetic Field in Late Wurm Ice Age

Izumi Yokoyama and Giovanni Napoleone*

Geophysical Institute, Hokkaido University

The authors and their colleagues are investigating various physical properties of pyroclastic deposits around Sikotu Caldera, Hokkaido. This is a preliminary report on a result of palaeomagnetic studies.

Around Sikotu Caldera, there is a tremendous amount of pyroclastic deposits in such modes as pumice fall, pumice flow and welded tuff and we can find pumice fall deposits of 1 meter thick even at a distance of 90 km from the caldera. In 1957, Y. Katsui (1958) discovered a fossil forest embedded in the pumice fall deposits near Bibi about 30 km distant from the caldera and dated some carbonized trees buried in pumice by means of ^{14}. as 18,000 years B.P. (late Wurm ice age) ; Sikotu Caldera was formed at this age.

The sampling site for palaeomagnetic studies is a cliff of about 20 meters in relative height at Tokiwa, near Sapporo, about 20 km northward from the caldera. This cliff is composed of welded tuff except its uppermost layer of a few meters in thickness. About 20 samples were collected every meter along the vertical slope of the cliff.

The directions of natural remanent magnetization (NRM) of these samples are almost normal, some of them being shown on Schmidt projection in Fig. 1 and their intensities are strongest at the middle part of the cliff where welding is also of the highest degree. The NRM of the samples from the middle part were studied by Thelliers' stepwise heating method (Thellier and Thellier, 1959) : thermal decay of the NRM J_n was compared with the

---

* Permanent address: Osservatorio Vesuviano, Resina (Napoli), Italy

partial acquisition of thermal remanent magnetization (TRM) J_t between room temperature and the Curie point. Their J_t is nearly proportional to J_n as shown in Fig. 2 for example. On the basis that the intensity of TRM is proportional to the applied field, the ratio between the intensity of the ancient field at the sampling site (F) and that of the present geomagnetic field at the laboratory (F_0 =0.465 Oe), is determined from the gradient of the J_n-J_t curves, of which an example is shown in Fig. 3. The four results so far obtained are as follows:

Sample No.	9	11	15	16
F/F_0	1.47	2.21	1.37	1.58

(Sample numbers derive from the depths from the top of the cliff.) The ratios are around 1.5 except No. 11. Such scattering of the measured values may be inevitable because pyroclastic deposits are not always uniform in their chemical compositions and density. Using this ratio F/F_0, we can normalize the observed J_t-curve as shown by a broken line in Fig. 2. The similarity between the normalized J_t-curve and the observed J_n-curve verifies the proportionality between the J_t and the J_n, and also means that the pyroclastics at the sampling site arrived there from the centre of eruptions with a temperature not lower than the Curie point: according to V. Bucha's experiments (1965), J_n-curves deviate very far from the normalized J_t-curves in the temperature range between the temperature of deposition and the Curie point when the former is lower than the latter.

We may conclude that the intensity of the earth's magnetic field at 18,000 years B.P. near Sapporo was as large as 1.5 times of the present one. In Japan, there is distributed a large amount of pyroclastic deposits around volcanoes and calderas, which usually contain some carbonized material and their ages were already determined by means of ^{14}C as 3000～33000 years B.P. (e.g. K. Kigoshi, 1965). The authors would like to note possible utility of these pyroclastic deposits for palaeomagnetic studies.

References

Bucha, V. (1965), Results of archaeomagnetic research in Czechoslovakia for the epoch from 4400 B.C. to the present, Journ. Geomag. Geoelectr., 17, 407-423.

Katsui, Y. (1958), On the fossil forest embedded in the Shikotsu pumice fall deposit, Hokkaido (in Japanese), Journ. Geology Japan, 64, 379-385.

Kigoshi, K. (1965), Methods of age-determination by radioactivity (in Japanese), p87, Kinokuniya (Tokyo).

Thellier, E. and Thellier, O. (1959), Sur l'intensité du champ magnétique terrestre dans le passé historique et géologique, Ann. Geophys., 15, 288-376.

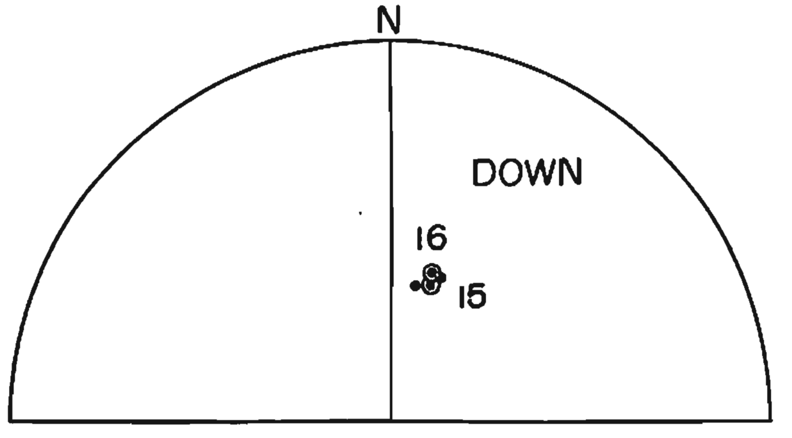

Fig. 1 Directions of the NRM of Sample Nos. 15 and 16.

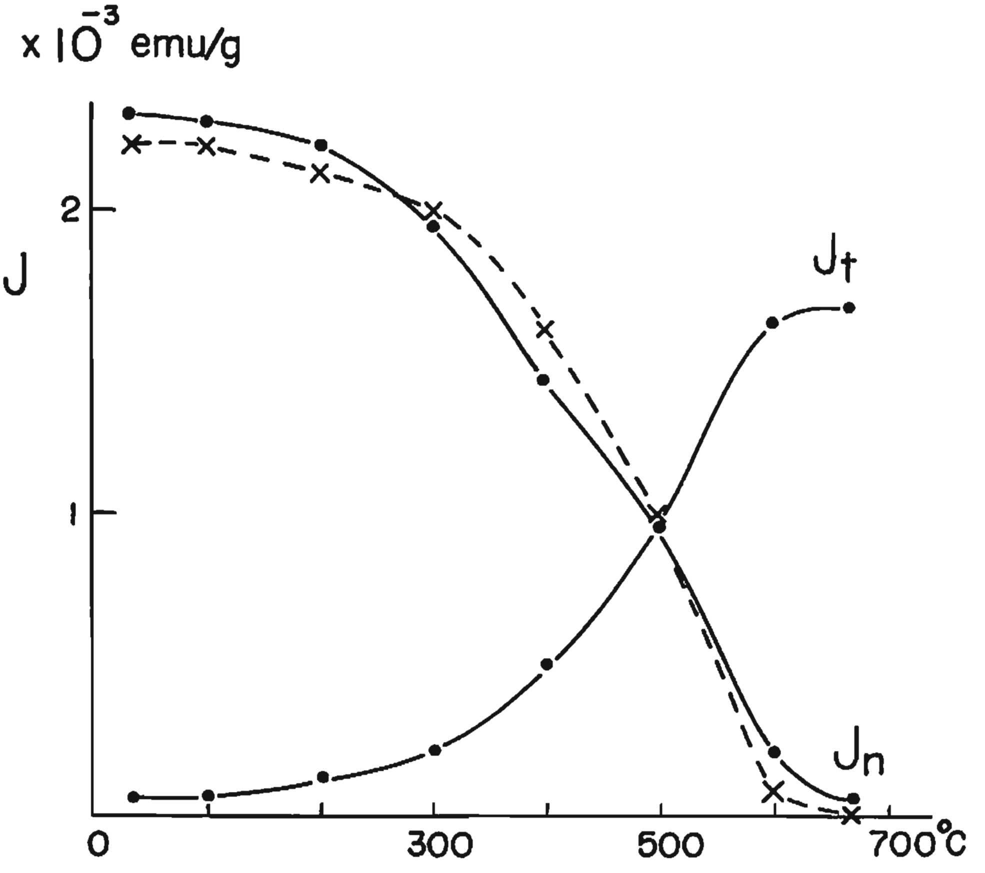

Fig. 2 Variations of J_n and J_t of Sample No. 15 versus temperature. Broken line shows the normalized J_t-curve.

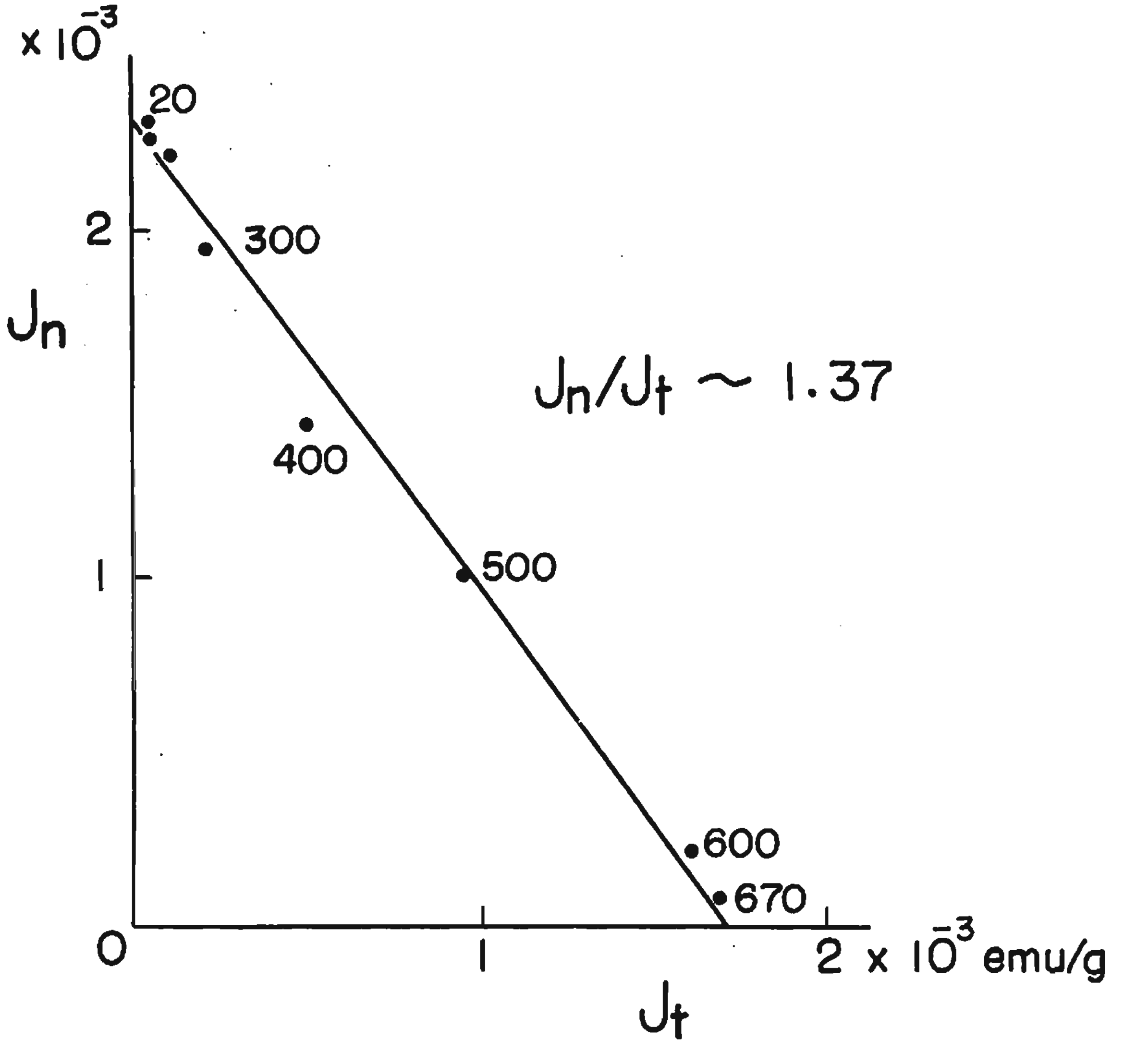

Fig. 3 $J_n - J_t$ curve of Sample No. 15. Numerals along the line indicate temperature in ℃.

7. Paleomagnetic Study in Southern Part of Hokkaido

Yasunori Nishida

Geophysical Institute, Hokkaido University

Some results of paleomagnetic study in a part of Southern Hokkaido and in the coastal region of the Okhotsk Sea were published by the present author (Nishida 1966, Nishida and Yokoyama 1965 and Nishida 1967). Recently, the samples of igneous rocks were collected from Hakodate-yama, southern limit of Hokkaido.

At Hakodate-yama, dacitic lavas and agglomerates are developed on the Samukawa volcanics which are considered as the upper Miocene. They are classified, according to their distributions and superpositions, into the five rock units as follows: Tachimachimisaki lava, Senjōjiki agglomerate, Kōryujiyama lava, Senjōjiki lava and Gotenyama lava. The age of their eruptions is supposed, judged from the degree of dissection inflicted on the volcano, to range from the late Neogene to the beginning of the Quaternary Period. The geological map is shown in Fig. 1. Samples were collected from Tachimachimisaki lava (sample No. 1), Kōryuji lava (No.2) and Samukawa volcanics (No.3). N.R.M.s of the samples were measured with a astatic magnetometer by the present author. The magnetic properties are summarized in Table 1 and the directions of N.R.M.s are protted on a Schmidt's diagram in Fig. 2. The age of the rock specimens from Hakodate-yama were presumed as the late Neogene because of the reversal magnetization, although the age is not distinguished whether the late Neogene or the beginning of the Quaternary by geological method. Paleomagnetic north poles calculated from the N.R.M. directions of the Hakodate-yama rock samples are protted in Fig. 3 which includes the data already published.

As already mentioned (Nishida 1966, Nishida and Yokoyama 1965 and Nishida 1967), the pole positions obtained from the samples collected from the coastal region of the Okhotsk Sea coinside with the pole path deduced from the southern part of Japan (e.g. Ito 1965), and the pole positions obtained from Sapporo region seem to constitute the different pole path travelling on South America during the upper Miocene-lower Pliocene period. The result from Hakodate-yama have also the same tendency with the latter case. And the pole positions seem to be dispersed at rather middle and low latitude along a certain pole path. On the other hand, the pole positions of the upper Pliocene deduced from the southern part of Hokkaido seem to be dispersed between the above two pole pathes during the upper Miocene-lower Pliocene period.

The above-mentioned difference of pole positions may possibly be attributed to the relative crustal movements in a large scale between the southern part of Hokkaido and the main island of Japan, even if N.R.M.s having pole positions on middle and low latitude were acquired during the rotation of geomagnetic dipole (Ito 1965). Such crustal movements may have not only rotational component but tilting, because the magnetic directions of the rock specimens sampled from the southern part of Hokkaido have rather large inclination whether plus or minus as already mentioned in previous papers. And such crustal instability in a large scale may relate with the tectonic movements after the Miocene.

On the other hand, there might be no large crustal movements at the coastal region of the Okhotsk Sea in comparison with the southern part of Hokkaido with the exception of up and down movements.

However, paleomagnetic data not only from Hokkaido but also from the eastern part of Japan are not so systematic that the problem of quantitative crustal movements can not yet be discussed. In order to settle this problem, the more investigations are required.

References

Nishida, Y. (1966), Paleomagnetic Study around Sapporo in Hokkaido (1st Paper), Geophys. Bull. Hokkaido Univ., 15. (in Japanese).

Nishida, Y., Yokoyama, I. (1965), Annual Progress Report of the Rock Magnetism Group.

Nishida, Y. (1967), Annual Progress Report of Paleogeophysics Research in Japan.

e.g. Ito, H. (1965), Paleomagnetic Study on a Granitic Rock Mass with Normal and Reverse Natural Remanent Magnetization, J. Geomag. Geoelect., 12.

Table 1. Various magnetic properties of the samples

Sample	Rock Kind	Direction		Pole Position		Intensity (10^{-4} emu/gr.)	
No. 1	Dacite	-72°	149°E	65°S	79°W	8	26
No. 2	Dacite	-59°	178°W	88°S	43°W	1	7
No. 3	Tuff-Agglomerate	-78°	150°E	60°S	62°W	5	11

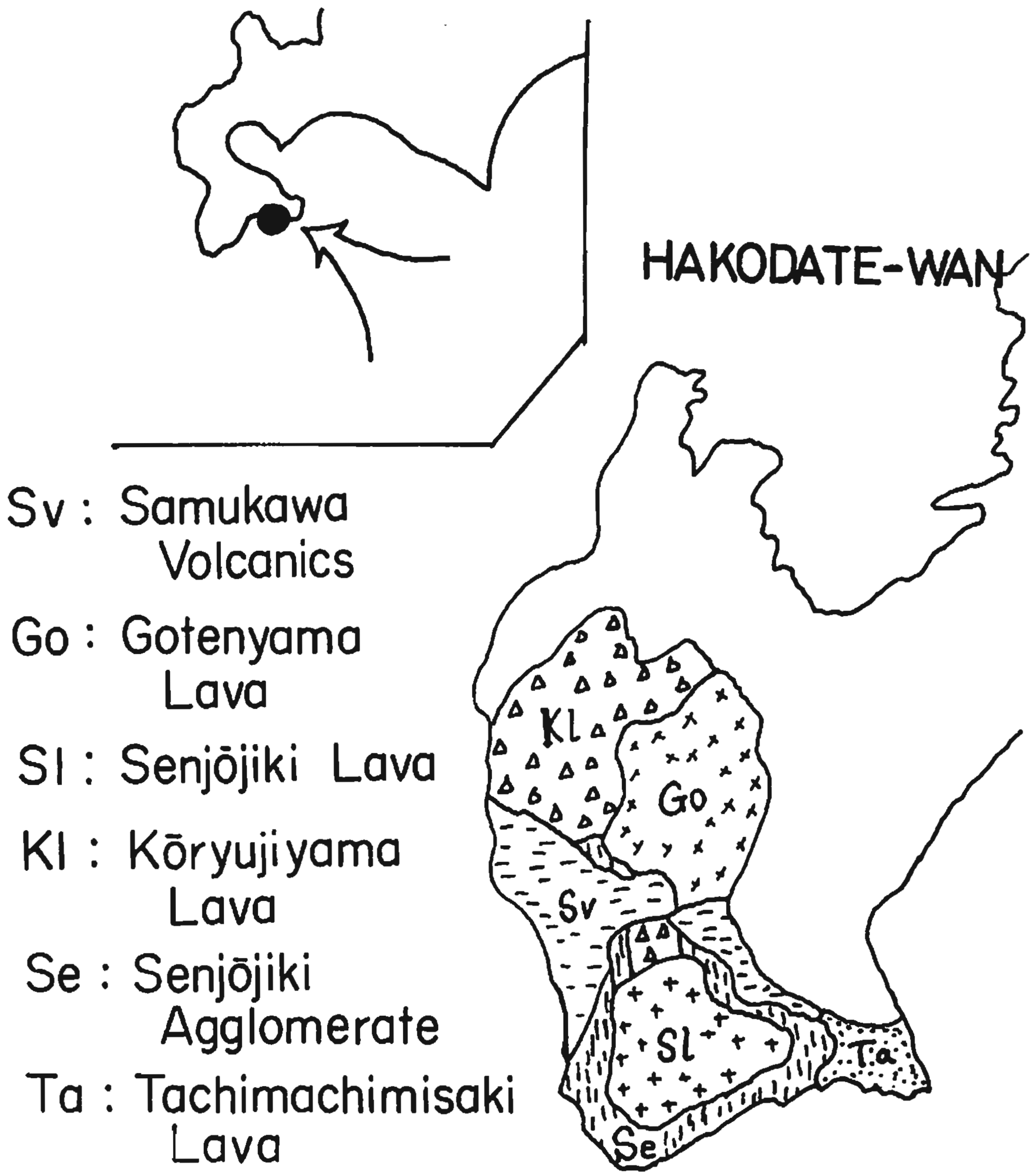
HAKODATE-WAN
Sv : Samukawa Volcanics
Go : Gotenyama Lava
Sl : Senjōjiki Lava
Kl : Kōryujiyama Lava
Se : Senjōjiki Agglomerate
Ta : Tachimachimisaki Lava
Kl
Go
Sv
Sl
Ta
Se

Fig. 1

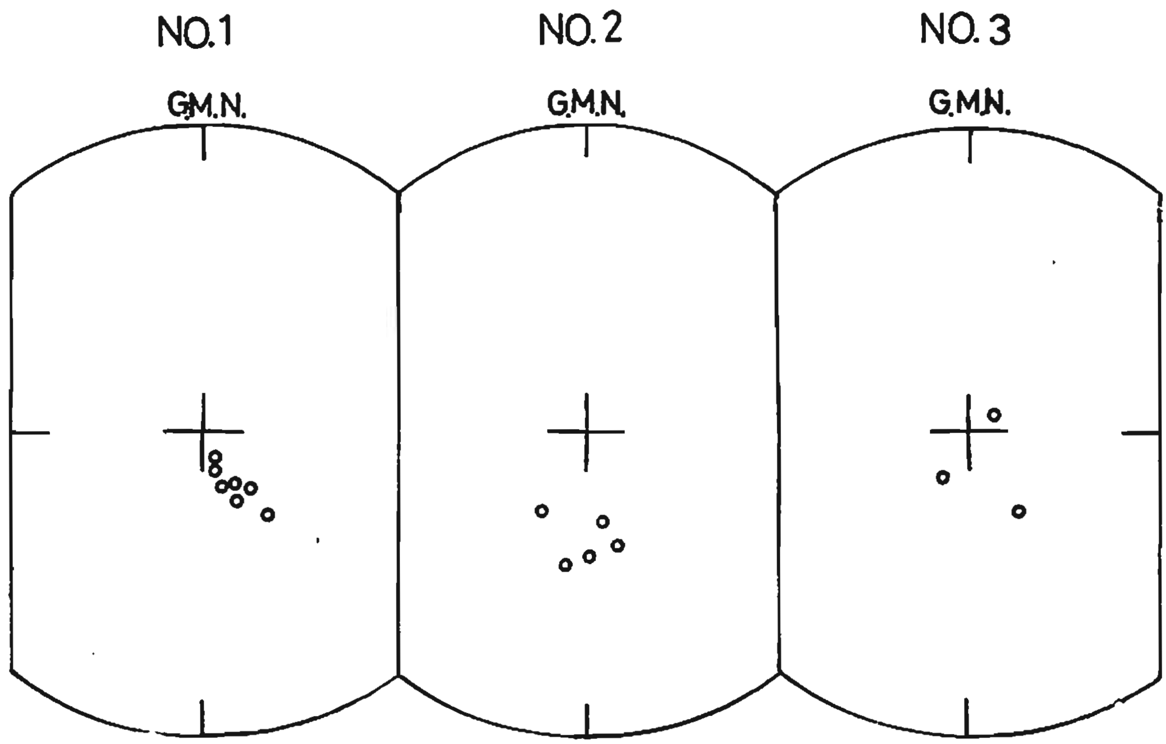

Fig. 2

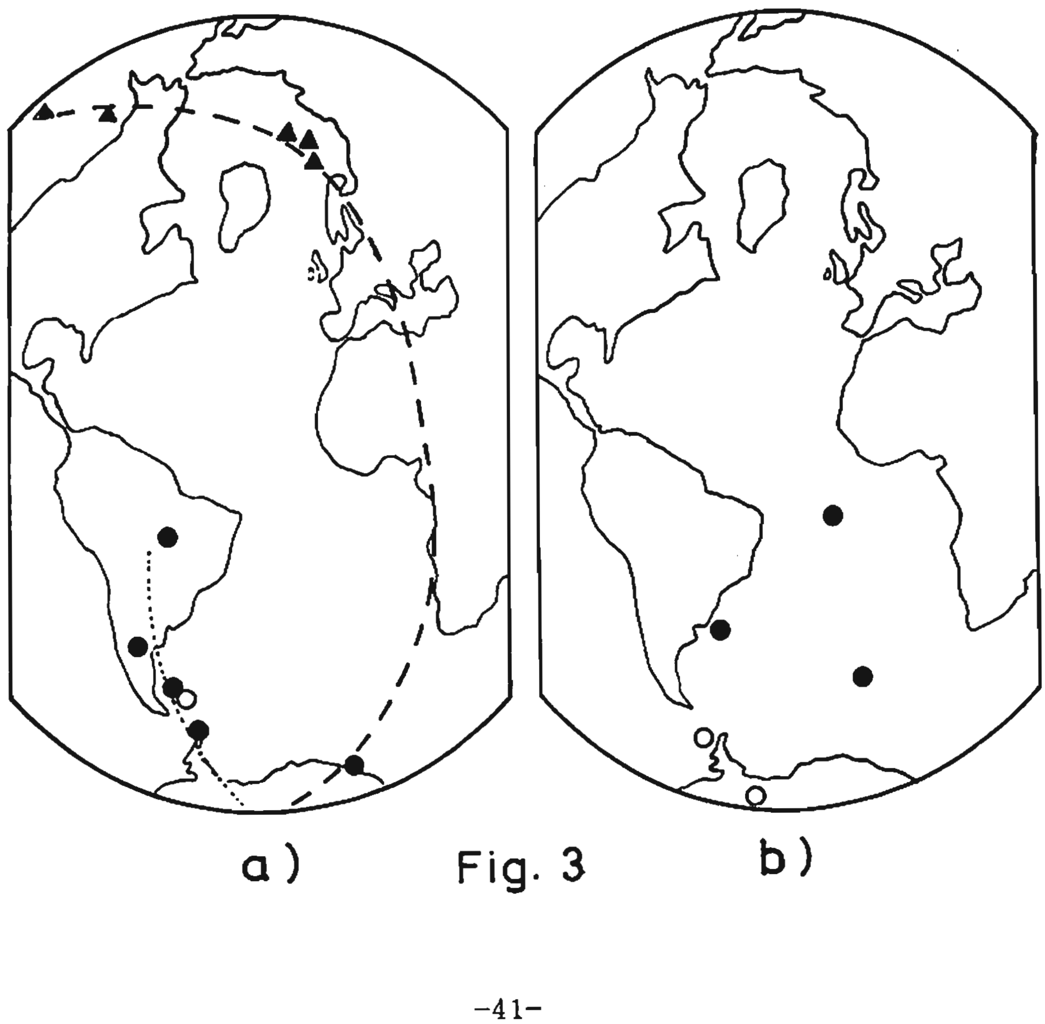

Fig. 3

8. The Paleomagneto-stratigraphic Correlation between Miocene Volcanic Series developed in Northeast and Southwest Japan

Sadao Sasajima and Junichi Nishida

Department of Geology and Mineralogy,

Kyoto University, Kyoto

Recently the authors have undertaken the paleomagnetic study of the Hokutan formations developed on the Japan Sea-side of the northern parts of Kyoto and Hyogo prefectures, Southwest Japan. The volcano-stratigraphic investigation of this group and its stratigraphic correlation with some nearby Miocene formations developed in the Japan Sea-side had been established by Wadatsumi et al. (1966). The formations, mostly composed of Miocene volcanic members, are little suffered from post-volcanic alterations usually affected the Miocene formations lying on the Japan Sea-side. More than 300 volcanic rock samples collected from 30 sites have been measured of their NRM before and after partial a.f. demagnetization of 100 to 200 Oe.

One of aims of the present study was to attempt the magneto-stratigraphic correlation between the Miocene magneto-stratigraphic columns obtained from Northeast and Southwest Japan. In other words, it implies to examine whether or not the paleomagnetic correlation by making use of the reversed zones of the Miocene volcanic series can be used successfully at present. There were three magneto-stratigraphic studies on the Miocene volcanic series which were separately distributed in Northeast Japan: Two of them were published by Nomura (1963, 1967), one from the Sendai district on the Pacific-side, and another from the Dewa Hill district on the Japan Sea-side, and the remaining one was obtained by Manabe (1967) from the Fukushima district on the Pacific-side.

Three reversed zones of NRM each in the early, middle and late Miocene were first found by Nomura from the Sendai district and the reversed zones were tentatively correlated with those reported from New Zealand (Coombs et al., 1959) and Europe (Hospers, 1955). Since then, in Dewa Hill district he has reported other three reversed zones presumably occupied different horizons from those of the three reversed zones mentioned above. However, in the same year Manabe reported that the three reversed zones found in his magneto-stratigraphic studies on the Fukushima district could be correlated with the three reversed zones obtained from the Sendai district, and that the reversed zone in the early Miocene was to be divided into two sub-zones in detail.

The obtained result of magneto-stratigraphic study of the Hokutan formations was far different from the initial purpose of the magnetic correlation by making use of reversed zones. It is meaningful to remind the reader of the paleomagnetic study of the Miocene Columbia Plateau basalts reported by Watkins (1965), who pointed out a difficulty of utilizing the paleomagnetic correlation between certain two distant sections. The present authors' idea has finally inclined to the opinion that such small number of reversed zones as three or four found by each investigator from the different basins in Japan can hardly be correlated with one another. This opinion may be easily accepted to everyone, if one take into account of the fact that only from a small fraction of the whole stratigraphic section is taken rock samples and measured their NRM polarity by all investigators.

The details of the paleomagnetic results will be published in the near future, but only the brief descriptions are given as follows:

1) Although the obtained magneto-stratigraphic succession was not so continuous to cover the entire column, there were found six reversed zones in the Hokutan formations; one is of the early Miocene age and five of the late Miocene age.

2) Stability tests of NRM for the paleomagnetic purpose were carefully

carried out, but only a few samples possessing less reliability were excluded from the data.

3) Averaged direction of site mean of NRMs is 2.0° E in declination and 55.4° in inclination, and its corresponding virtual pole position in the northern hemisphere lies at the coordinate, 175.7° E long., 87.8° N lat., showing a good accordance with the present North Pole.

In order to correlate the magneto-stratigraphic column of the Hokutan formations with those obtained from Northeast Japan by different authors, the present authors attempted to fit those stratigraphic columns into the absolute time scale. For this purpose two published correlation tables are available at present. One of them was reported by Chinzei (1967), and the other has been published very recently by Ikebe and Chiji (1969). Although those correlations cannot be said to be decisively established, they are highly helpful for the purpose of standardizing the local stratigraphic sequences into the absolute ages with a certain confidence level. In the diagram of Fig. 1 the stratigraphic correlation is referred in principle to the study by Ikebe et al., who have comprehensively unified the relation between the Neogene biostratigraphy and the K-Ar age data so far reported. Further K-Ar age data with known polarity shown in the figure are referred to the studies by Hirooka et al. (1967) and Kwano et al. (1964, 1966) on some igneous rocks in Japan.

If one could assume complete horizontal correlation among the reversed zones in the figure within the possible errors of the stratigraphic correlation, there may appear eight reversed zones during the Miocene epoch. On the contrary, the extreme case of no internal correlation among them leads to the maximum number of 16 reversed zones. These both cases are thought to be the extreme ones, therefore, the actual number of frequency may be expected to lie between them. However, it may be much proper to suppose that even the maximum number of 16 is still considerably smaller than the cycle of reversed zones presumably occurred during the Miocene. The reason is apparent from the fact that only a small fraction of the whole stratigraphic section was sampled and studied by all of the investigators.

Further, it cannot be denied that there remains the possibility of miscalculation of a few additional reversals supposedly existed within time gaps of slight unconformities which might be intercalated among volcanic layers. On the contrary, it must be considered, to a certain extent, that a few of 16 reversed zones might be truly correlated with each other; if this is the case, the corresponding number of subtraction from 16 should be made. As the consequence, it can probably be said that the possible increment of number of reversed zones are much larger than the decrement as mentioned above, thus resulting in net increase of the most likely number of reversed zones throughout the Miocene epoch.

In conclusion, it is suggested that the frequency of reversals in geomagnetism during the Miocene epoch is not significantly different from that for the past 4 m.y. and hence the paleomagnetic correlation by making use of the reversed zones is quite uncertain to be successfully applied. Further decisive magneto-stratigraphic studies are desired to examine the propriety of the geomagnetic polarity time scale in the Miocene epoch which was presented by Heirtzler et al. (1968), basing on the hypothesis of ocean floor spreading and the marine magnetic linear anomalies observed over the ocean ridges.

References

Chinzei, K. (1967), An attempt of fitting the stratigraphic correlation table of the Japanese Neogene systems into the absolute time. (in Japanese); Jour. Geol. Soc. Japan, 73, 220-221.

Coombs, D. S. and Hatherton, T. (1959), Paleomagnetic studies of Cenozoic volcanic rocks in New Zealand. Nature, 184, 883-884.

Heirtzler, J. R., G. O. Dickson, E. M. Herron, W. C. Pitman, III, and X. Le Pichon (1968), Marine magnetic anomalies, geomagnetic field reversals and motions of the ocean floor and continents. Jour. Geophys. Res., 73, 2119-2136.

Hirooka, K. and N. Kawai (1967), Results of age determination of some late Cenozoic rocks in Southwest Japan. 1967 Ann. Prog. Rept. Paleogeophysics Res., Osaka, 69-73.

Hospers, J. (1955), Rock magnetism and polar wandering. Jour. Geol. 63, 59-74.

Ikebe, N. and M. Chiji (1969), Neogene biostratigraphy and the "absolute age". (in Japanese with English abstract). Bull. Jap. Assoc. Petro. Technologists (in press).

Kawano, Y. and Y. Uyeda (1964), K-Ar dating on the igneous rocks in Japan (I). Jour. Japan Assoc. Min. Petro. Econ. Geol. 51, 127-148.

Kawano, Y. and Y. Uyeda (1966), K-Ar dating on the igneous rocks in Japan (IV). Jour. Japan Assoc. Min. Petro. Econ. Geol., 56, 41-55.

Manabe, K. (1967), Results of paleomagnetic studies on Miocene volcanic rocks in the Fukushima district, Northeast Honshu, Japan (in Japanese with English abstract). Jour..Geol. Soc. Japan, 73, 325-336.

Nomura, S. (1963), Paleomagnetic studies on the Neogene volvanic rocks from the Sendai district, Northeast Honshu, Japan. Earth Science, Tokyo, No. 67, 30-39 and No. 68, 22-27.

Nomura, S. (1967), On the properties on the paleomagnetic polarity of the Neogene and Quaternary volcanic rocks in Japan. Jour. Lib. Arts. Sci., Gunma Univ., 1, 11-35.

Wadatsumi, K., N. Ikebe and T. Matsumoto (1966), Correlation of the Neogene formations of Northern Kinki, Southwest Japan (in Japanese with English abstract). Memo. Volume, Professor S. Matsushita, Kyoto Univ., 105-116.

Watkins, N. D. (1965), Paleomagnetism of the Columbia Plateaus. Jour. Geophys. Res., 70, 1379-1406.

Figure Caption

Fig. 1. A chart showing the magneto-stratigraphic correlation of some Miocene Series studied in Japan, and the summarized polarity time changes during the epoch. ∧∧∧∧ , unconformity; _____, conformity; ----, not so well defined time-boundary; F., formation; M., member; *, standard stratigraphic division (stage) in Northeast Japan; numeral enclosed inside brackets indicates the number of site(s) studied. A, Ashizuri-misaki granite; Mi, Mikasayama Andesite; Mu, Muro dacite; K. Kumano acid rocks; N, Nijio dacite; O, Osumi granite; T, tanigawa-dake granite; W, Wakurayama Andesite.

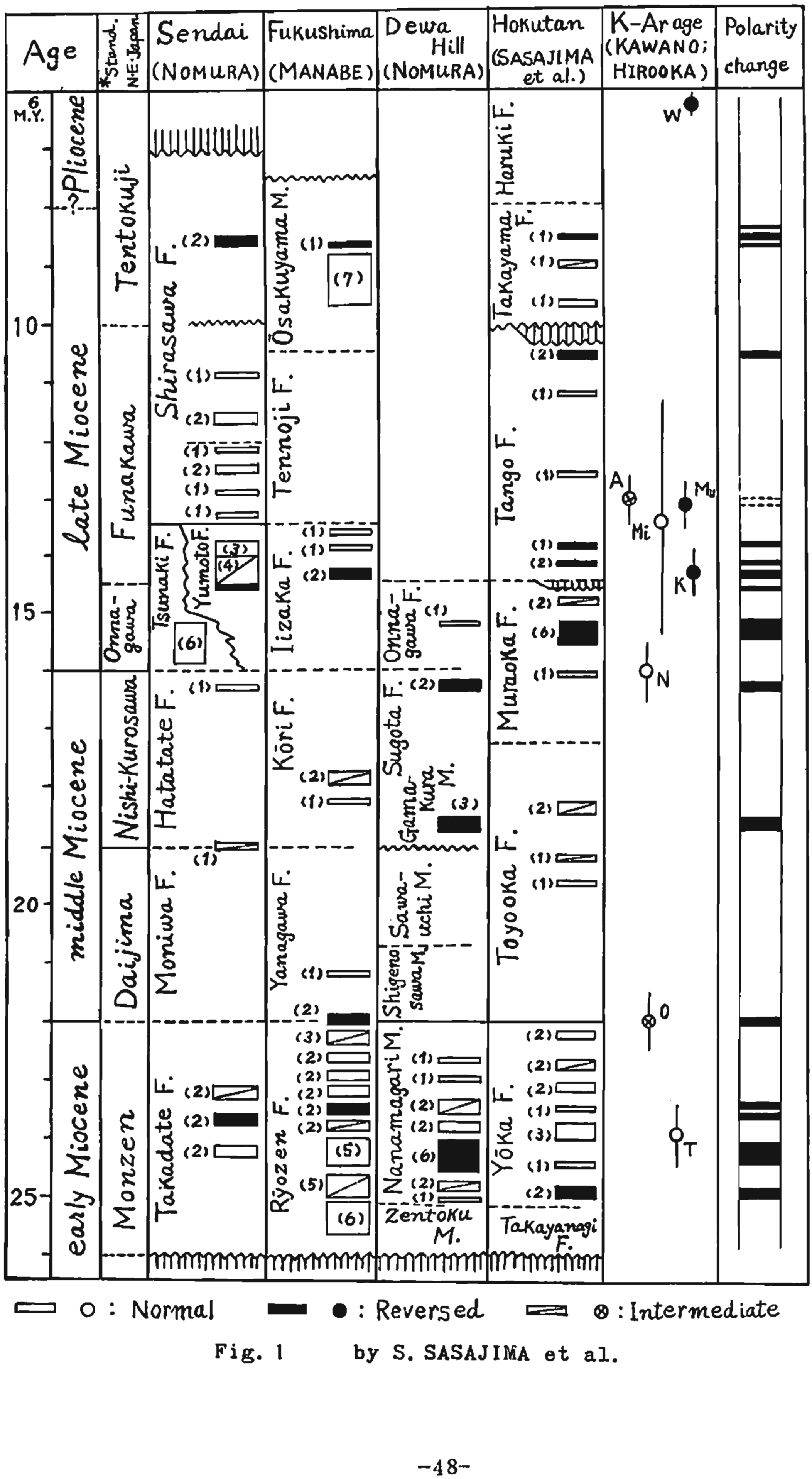

Fig. 1 by S. SASAJIMA et al.

9. Palaeolatitude of the Japanese Islands in the Palaeozoic and Mesozoic and its Bearing on Crustal Movement

Masao Minato and Yoshiki Fujiwara
Department of Geology, Hokkaido University

So far as the available data on palaeomagnetic studies, palaeolatitude of the Japanese islands seems to have been smoothly changed from north to south through Devonian to Triassic age. It had also been gradually shifted northward from the Triassic to the end of the Cretaceous.

The changing of latitude through geological ages seems to be well harmonized with the climatic change of the Japanese islands postulated from the palaeoclimatic data, as is previously reported by Minato and Fujiwara (1964).

In Fig. 1, black circle means the palaeolatitude postulated from the rocks sampled either in the northern Honshu or Hokkaido, while the white circle either from the southwestern Honshu or Kyushu based on the palaeomagnetic data as Nagata et al. (1959, 1960), Sasajima and Shimada (1966), Ueno (1967) and present authors.

As in shown in Fig. 1, the shift of palaeolatitude of the Japanese islands through geological ages suggests that it have been occured in the past with a certain regularity. Namely, the Middle Devonian is 43°N, Lower Carboniferous Tournasian : 20°N, Namurian : 17°N, Lower Permian : 10°N and Late Triassic : 5°N.

The Palaeolatitude postulated from the rocks sampled from the southern Japan as not show any meaningful fluctuation for the age ranging from the Cenomanian until the Palaeogene, while the palaeolatitude shown by the rocks from the northern Japan seems to have been ever shifted northward from the Aptian until the Palaeogene through the end of the Cretaceous.

Therefore, it is believed that the rate of horizontal shifting and its direction might become different between northern and southern part of Japan since the Middle Cretaceous. The horizontal movement may have been more stronger in the northern half compared to the southern part during the Late Cretaceous and Palaeogene. Fig. 2 shows the presumed palaeogeographic position of the Japanese islands in Early Cretaceous based on the present palaeomagnetic study.

References

Minato and Fujiwara (1964), Proc. Japan Acad., Vol. 40, No.2, 116-120.

Nagata et al. (1959), Proc. Japan Acad., Vol. 35, 378-383.

Sasajima and Shimada (1966), Jour. Geol. Soc. Japan, Vol. 72, No. 10, 503-514.

Kang (1966), The Korean Sci. Inform. Vol. 3, No. 6.

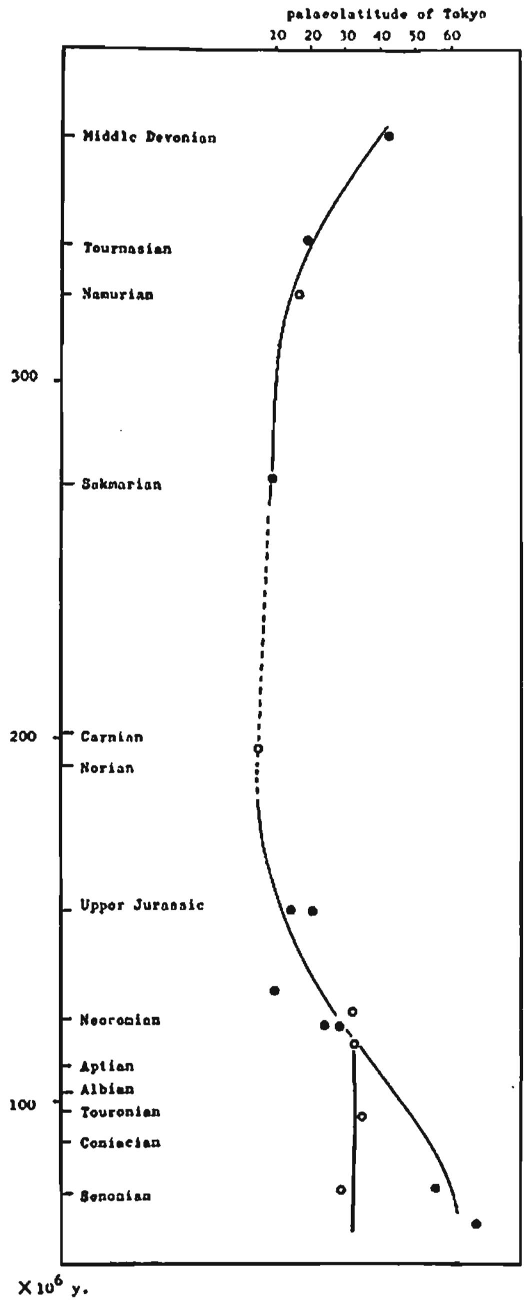

Fig. 1 Changing of the palaeolatitude of Tokyo through the Palaeozoic and Mesozoic estimated from the palaeomagnetic studies on the Japanese rocks. Time scale is based on the Holm's symposium volume (1964).

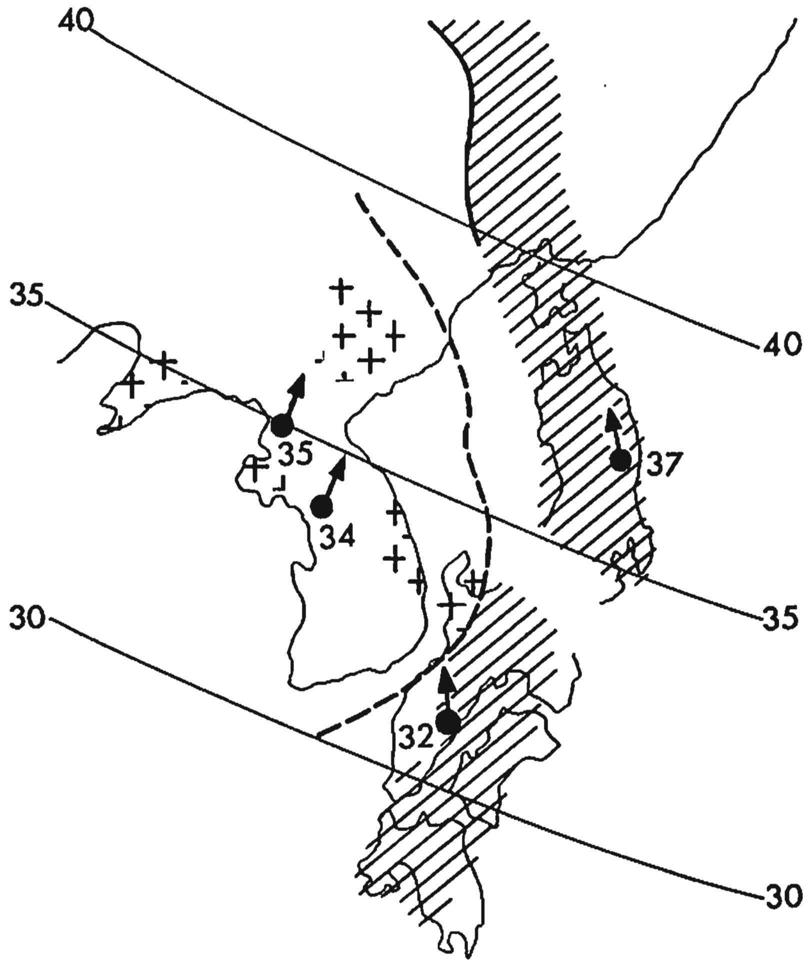

Fig. 2 The supposed palaeogeographic position of the Japanese islands in the Late Mesozoic infferred from palaeomagnetic data. Cross area shows the pressumed land mass in the Late Palaeozoic to the Early Cretaceous. The shaded portion of the map is Palaeozoic geosynclinal area. The arrows give the declination. Data in Korea are from Kang (1966).

10. Thermodynamic Estimation of the Physical Conditions on the Formation of Some Plutonic Nodules —— An Application of the Theory on the Equilibrium Distribution ——.

Takashi Matsumoto

Institute for Thermal Spring Research

Okayama University

Misasa, Tottori-Ken, Japan

It is possible in principle to determine simultaneously the temperature and the pressure at equilibrium of a definite solid solution pair by combining at least two of the appropriate exchange reaction, as has been pointed by Matsui and Banno (1967).

By means of the thermodynamic analysis along the principle mentioned above on the equilibrium distribution of Mg, Fe, and Co between the olivine solid solution and the orthopyroxene solid solution coexisting in an ultramafic rock, we can estimate the physical condition at equilibrium of that mineral pair, wherein we must combine the following two of the exchange reaction:

$$MgSi_{0.5}O_2 + FeSiO_3 = FeSi_{0.5}O_2 + MgSiO_3 \quad \ldots\ldots\ldots\ldots\ldots \quad (1)$$

and

$$MgSi_{0.5}O_2 + CoSiO_3 = CoSi_{0.5}O_2 + MgSiO_3 \quad \ldots\ldots\ldots\ldots\ldots \quad (2)$$

If we can apply the binary regular solution model, the apparent partition coefficient K_D^{Fe-Mg} in the equilibrium distribution of Fe and Mg between Mg-Fe olivine and Mg-Fe orthopyroxene must have the following form of expression:

$$R\cdot T\cdot \ln K_D^{Fe-Mg} = -\Delta G_1 + (1-2X_{Mg})_{ol} \times (W^{ol}_{Mg-Fe} \times P + \alpha^{ol}_{Mg-Fe}) - (1-2X_{Mg})_{opx} \times (W^{opx}_{Mg-Fe} \times P + \alpha^{opx}_{Mg-Fe}) \ldots (3),$$

wherein

G_1 : the free energy of the reaction (1), the value of which is obtained as the function of temperature and pressure by combining Kelley's data and the free energy of reaction in $FeSi_{0.5}O_2+Si_{0.5}O=FeSiO$, determined experimentally by Akimoto, Katsura, Syono, Fujisawa and Komada (1965),

T : temperature$^{\circ}$k, P : pressure, and X_{Mg} : molal fraction of Mg.

Utilizing redox reaction, Nafziger and Muan (1967) have estimated the true partition coefficient in the equilibrium distribution of Mg and Fe between paragenetic Mg-Fe olivine and Mg-Fe orthopyroxene, and have shown that these solid solutions were well approximated by the binary regular solution model.

According to their data, the calorimetric term of the characteristic parameter of Mg-Fe olivine solid solution represented by α^{ol}_{Mg-Fe} is calculated to be 1100cal/mol —— 1200cal/mol and that of Mg-Fe orthopyroxene solid solution represented by α^{opx}_{Mg-Fe} is calculated to be 600cal/mol —— 700cal/mol respectively; the volumetric term of the same parameter of the olivine represented by W^{ol}_{Mg-Fe} is calculated to be about +0.12c.c./mol and that of the orthopyroxene W^{opx}_{Mg-Fe} is calculated to be about -0.17c.c./mol according to the cell parameter data given by Matsui, and Syono (1968).

Since each of the molal fraction of Mg or Fe in the olivine solid solution and in the orthopyroxene solid solution found in an ultramafic rock is exclusively large, Eq. (3) may be applied to the olivine-orthopyroxene pair in an ultramafic rock.

The equilibrium distribution of Mg and Co in the olivine-orthopyroxene pair in an ultramafic rock must be approximated on the basis of ternary regular solution model. In this case, however, since Mg-Co olivine and Mg-Co orthopyroxene solid solutions may be taken as ideal solution according to the cell parameter data given by Matsui, and Syono (1968), and since the molal fraction of Mg or Fe in the olivine solid solution has roughly the same value with that of the orthopyroxene in an ultramafic rock, apparent partition coefficient K_D^{Co-Mg} must have the following form of expression:

$$RT\ln K_D^{Co-Mg} = -\Delta G_2 - X_{Fe}\times(\Delta\alpha_{Mg-Fe} + \Delta W_{Mg-Fe}\times P) - X_{Mg}\times X_{Fe}\times(\Delta\alpha_{Mg-Fe} + \Delta W_{Mg-Fe}\times P)$$

.... (4) and $\Delta\alpha_{Mg-Fe} = \alpha^{ol}_{Mg-Fe} - \alpha^{opx}_{Mg-Fe}$, $\Delta W^{ol}_{Mg-Fe} = W_{Mg-Fe} - W^{opx}_{Mg-Fe}$

wherein

ΔG_2 : the free energy of the reaction (2), which is calculated by combining Kelley's data and the free energy of reaction in

$$CoSi_{0.5}O_2 + Si_{0.5}O = CoSiO_3$$ given by Akimoto et al. (1965).

As a result, if we know K_D^{Fe-Mg} and K_D^{Co-Mg} by the chemical analysis of the mineral pair in interest, we can obtain the physical condition at equilibrium of an ultramafic rock by combining Eq. (3) and (4).

As an example, the physical conditions at equilibrium of the mineral pair about the lherzolite sampled at the Ichinomegata-maar, Japan; and about the kimberlite sampled at the Dutoitspan-pipe, South Africa are determined respectively, where K_D^{Fe-Mg} and K_D^{Co-Mg} in these mineral pairs are obtained on the basis of the data given by Ross, and Foster (1954) and by Matsui (1968).

For the most possible values of $\alpha's_{Mg-Fe}$ and $W's_{Mg-Fe}$, the estimated pressure for the Ichinomegata-lherzolite comes to be 10 kb±, and that for the Dutoitspan-kimberlite comes to be 40 kb±. These values might mean the pressures, at which these rocks have been formed; especially, the later value is well consistent with the delineated one, which has been concluded from the high pressure experiment on the later sample performed by Ito, Matsumoto, and Kawai (1968).

In conclusion, I would like to insist the importance of the thermodynamic data and the cell parameters of such minerals as $CoSi_{0.5}O_2$ and $CoSiO_3$, which are not found as pure phases in nature, for the purpose of the estimation of the physical conditions on the formation of plutonic nodules.

References

Akimoto, S., T. Katsura, Y. Syono, H. Fujisawa, and E. Komada (1965): Polymorphic Transition of Pyroxenes $FeSiO_3$ and $CoSiO_3$ at High Pressures and Temperatures. Jour. Geophys. Res., 70, no. 20, 5269-5278.

Matsui, Y., Y. Syono, (1968): Unit cell dimensions of some synthetic olivine group solid solutions. Geochemical Jour., 2, 51-59.

Matsui, Y., Y. Syono, S. Akimoto, and K. Kitayama (1968): Unit cell dimensions of some orthopyroxene group solid solutions. Geochemical Jour., 2, 61-70.

Nafziger, R. H., and A. Muan (1967): Equilibrium Phase Compositions and Thermodynamic Properties of Olivines and Pyroxenes in the System MgO-"FeO"-SiO_2. Amer. Miner., 52, 1364-1385.

Prigogene, I., and R. Defay (1954): Chemical Thermodynamics. Longmans Green, London.

Ross, C. S., M. D. Foster, and A. T. Meyers (1954): Origin of Dunites and of Olivinerich Inclusions in Basaltic Rocks. Amer. Miner., 39, nos. 9 & 10, 693-737.

11. Graphical Interpretation of PRM for Single-domain Grains

D. J. Dunlop, M. Ozima and H. Kinoshita
Geophysical Institute, University of Tokyo

Rock magnetists are well-acquainted with the classic Néel (1949) theory of single-domain grains, which interprets TRM as a magnetization blocking process: grains preserve at room temperature a remanence which was "frozen-in" at the blocking temperature. Demagnetization, either by heating or by an alternating field, is a magnetization relaxation or "unblocking" process. Since Neel's equations for relaxation time include the effects of time, t, and magnetic field, H, as well as temperature, magnetic viscosity, isothermal remanence (IRM) and anhysteretic remanence (ARM) can be treated in an analogous way to TRM. The correctness of these interpretations has recently been verified experimentally (Dunlop, 1968; Dunlop and West, 1969).

In this paper, we will show how the Neel theory can be extended in a simple way to analyse irreversible piezomagnetic processes, such as piezoremanent magnetization (PRM) and pressure demagnetization, in the experimentally interesting case of a uniaxial stress σ parallel to the applied magnetic field H. Essentially, in Néel's equations for the relaxation time of a grain of microscopic coercive force H_c and volume v, H_c is replaced by $H_c - 3\lambda\sigma/J_s$ (λ is saturation magnetostriction, J_s is spontaneous magnetization).

The Néel diagram (Neel, 1949), illustrated in Fig. 1, is an extremely useful device for visualizing magnetization (TRM, IRM, ARM, VRM) and demagnetization (AF and thermal demagnetization, magnetic viscosity) in single-domain samples. Each grain of such a sample has a representative point (v, H_{co}) on the diagram, H_{co} being the value of H_c at 20°C. Under any set of experimental conditions (H, T, σ, t), Neel's relaxation time equation can be plotted as a "blocking curve" on the diagram. Since the blocking curve expresses the condition $\tau = t_{exp}$ (τ is relaxation time, t_{exp} is the time of an experiment), grains to the left and below the curve are unblocked ($\tau \ll t_{exp}$) while those above and to the right are blocked ($\tau \gg t_{exp}$). A change in experimental conditions causes the blocking curve to move, blocking or unblocking the grains through which it passes.

Fig. 1(a) shows a series of blocking curves at various temperatures. Increasing temperature moves the 20°C curve up and to the right, progressively unblocking the grains which carried stable remanence at 20°C: by this model we can analyse thermal demagnetization. The same set of blocking curves can be used to analyse the progressive acquisition of TRM. The blocking curve motion is of course reversed in this case; grains become blocked and acquire a remanence as the curve passes through them. Isothermal processes involving changing magnetic field (IRM, ARM, AF demagnetization) are modelled in an analogous way by the blocking curves of Fig. 1(b). Motion to the right, as indicated by the arrow, corresponds to AF demagnetization in progressively larger fields.

Blocking curves suitable for analysing PRM and pressure demagnetization are shown in Fig. 1(c). Since the effect of σ is to decrease H_{c} by $3\lambda\sigma/J_s$, the blocking curve motion is parallel to the H_{co} axis and proportional to σ.

Intensity of PRM

Experimentally, the intensity of PRM depends on the order in which σ and H are applied and removed. We will use Nagata and Kinoshita's (1965) notation H_+ and H_0 (or σ_+ and σ_0) to indicate applying and removing field (or stress). Our model for the remanence $J_r(H_+\sigma_+\sigma_0 H_0)$ or $J_r(\sigma_+ H_+ \sigma_0 H_0)$ is shown in Fig. 2(a). The processes $\sigma_+ H_+$ and $H_+\sigma_+$ are equivalent: both move the blocking curve from (0,0) to (σ,H). When σ is removed, the area between (σ,H) and (0,H) acquires a remanence in field H, and when H is removed at zero stress, the area between (O,H) and (O,O) becomes magnetized in a field which varies from H for grains near (O,H) to zero near (O,O). Obviously $J_r(H_+\sigma_+\sigma_0 H_0)$ or $J_r(\sigma_+ H_+\sigma_0 H_0)$ is larger than the ordinary IRM (shown as region 1 in Fig. 2(b)), which is localized between (O,H) and (O,O). It is also larger than $J_r(\sigma_+ H_+ H_0\sigma_0)$ or $J\ (H\sigma_+ H_0\sigma_0)$, shown as region 2 in Fig. 2(b): removing H in the presence of produces a remanence in the area between (σ,H) and (σ,O), but removing σ produces no further remanence because there is no magnetizing field during this latter process. These predictions are borne out by the experiments of Nagata and Kinoshita (1965).

The area swept out by the blocking curve is proportional to σ, so that we might expect $J_r(H_+\sigma_+\sigma_0 H_0)$ to be proportional to σ for small H. However, since the density of grains varies from place to place on the Neel diagram, the true $J_r(H_+\sigma_+\sigma_0 H_0)-\sigma$ relationship, as observed experimentally, is non-linear and is closely related to the coercivity spectrum of the sample. The Néel diagram picture, however, fails to predict the observed linear dependence of $J_r(H_+\sigma_+\sigma_0 H_0)$ on H (Domen, 1962; Nagata and Kinoshita, 1965; Nagata and Carleton, 1968).

Stability of PRM

Fig. 1(b) indicates that distance of a grain to the right of the v axis on the Néel diagram is an indication of its stability against AF demagnetization. Using this criterion, we can deduce from Fig. 2 that the average AF stability of $J_r(H_+\sigma_+\sigma_0 H_0)$ or $J_r(\sigma\ H_+\sigma_0 H_0)$ is greater than that of $J_r(H_+H_0)$ but less than that of $J_r(H_+\sigma_+ H_0\sigma_0)$ or $J_r(\sigma_+ H_+ H_0\sigma_0)$. Using the blocking curves of Fig. 1(a) and (c), we deduce that the same relation applies in the case of thermal or pressure demagnetization.

Furthermore, TRM and ARM, since they magnetize the entire Néel diagram, should have higher average stability than either IRM or PRM, leading to the general stability relationship

$$J_{ir} < J_r(H_+\sigma_+\sigma_0 H_0) < J_r(\sigma_+ H_+ H_0 \sigma_0) < J_{trr} \quad J_{nr}$$

for demagnetization by heating, by alternating fields or by compression. Currently available data on pressure demagnetization (Ohnaka and Kinoshita, 1968; Shimada et al., 1967) are in general agreement with this conclusion but more experiments are clearly called for.

This work was first reported at the Sendai meeting of the Society of Terrestrial Magnetism of Japan, 30 October 1968. A more detailed paper will be published soon.

References

Domen, H. (1962), J. Geomag. Geoelec. 13, 66.

Dunlop, D. J. (1965), ibid. 17, 459; (1968), Science 162, 256.

Dunlop, D. J. and G. F. West (1969), Rev. Geophys., in press.

Nagata, T. and B. J. Carleton (1968), J. Geomag. Geoelec. 20, 115.

Nagata, T. and H. Kinoshita, (1965), ibid. 17, 121.

Neel, L. (1949), Ann. Geophys. 5, 99.

Ohnaka, M. and H. Kinoshita (1968), J. Geomag. Geoelec. 20, 93.

Shimada, M., S. Kume and M. Koizumi (1967), in Annual Progress Report of Palaeogeophysics Research in Japan, p.117.

Figure Captions

Fig. 1. The Neel diagram and the motion of blocking curves with increasing (a) temperature, T, (b) magnetic field, H, and (c) uniaxial compressional stress, σ. Approximate values of T, H, and σ for magnetite are given on the curves.

Fig. 2. Representation of IRM and different types of PRM on the Neel diagram. Hatched areas represent: (a) $J_r(H_+\sigma_+\sigma_0 H_0)$ or $J_r(\sigma_+ H_+ \sigma_0 H_0)$; (b), region 1, IRM or $J_r(H_+ H_0)$; and (b), region 2, $J_r(\sigma_+ H_+ H_0 \sigma_0)$ or $J_r(H_+\sigma_+ H_0 \sigma_0)$.

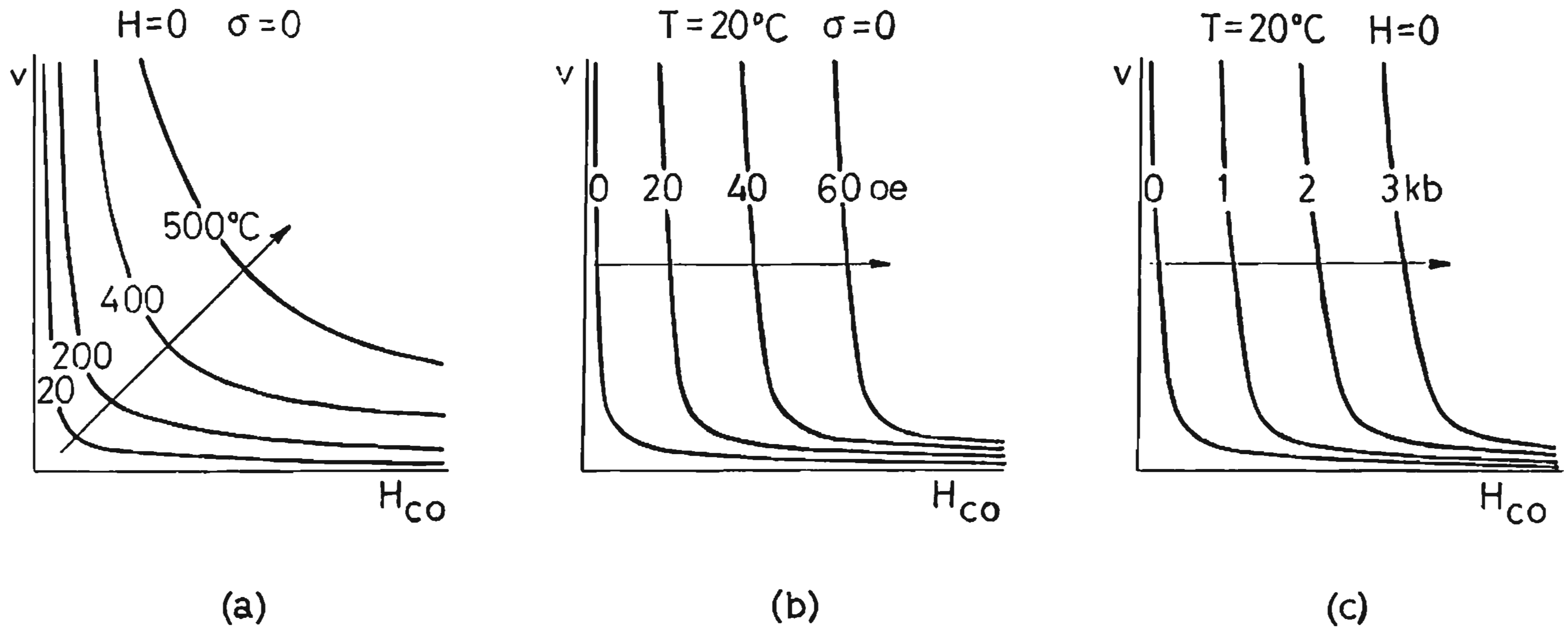

Dunlop, Ozima & Kinoshita Fig. 1 (of 2)

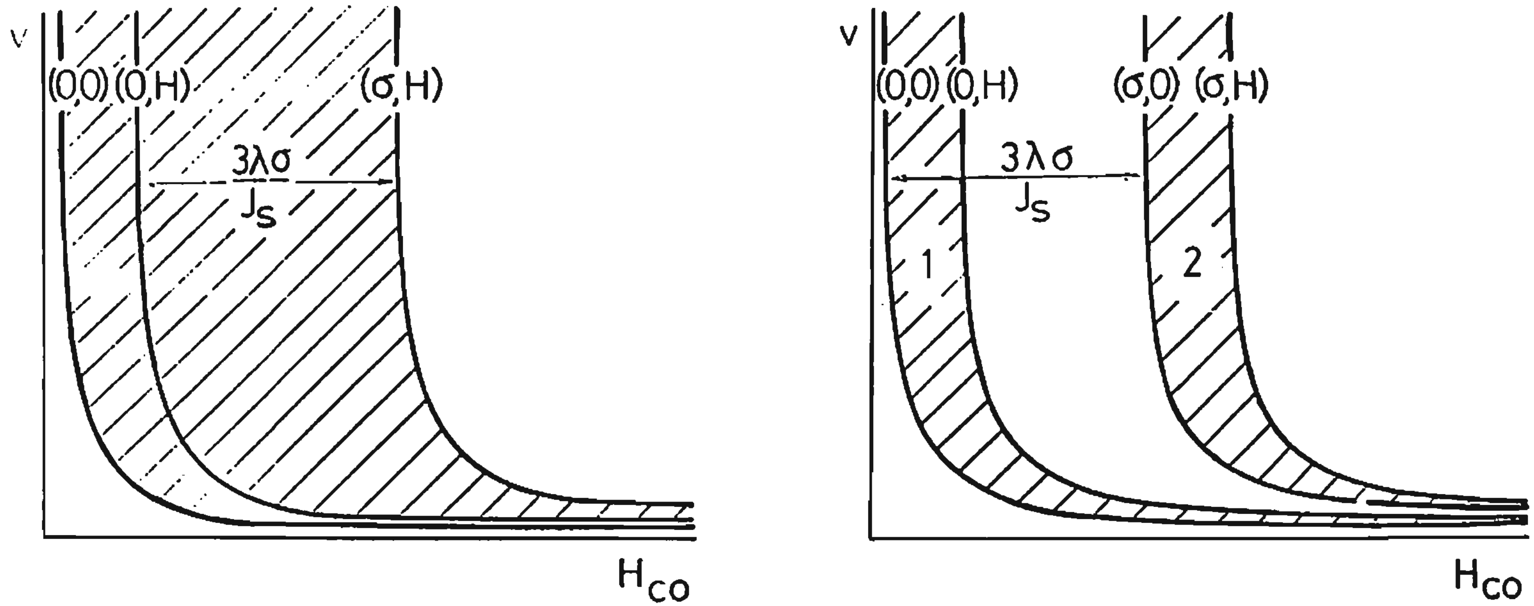

(a)

Dunlop, Ozima & Kinoshita Fig. 2 (of 2)

(b)

12. A Study of the Parasitic Ferromagnetism of Hematite between -196°C and 710°C

D. J. Dunlop

Geophysical Institute, University of Tokyo

The parasitic ferromagnetism of antiferromagnetic hematite has been studied by physicists for many years. It is now well established that between the Morin transition (-20°C) and the Curie point (675-680°C) the two spin sublattices are slightly canted out of perfect antiparallelism, giving rise to a small ferromagnetic moment in the basal plane (Dzialoshinskii, 1958; Moriya, 1960). Below -20°C, the spins lie along the c-axis and the spin-canting is very slight. However, some workers (Neel and Pauthenet, 1952; Lin, 1960) report a small low-temperature moment observable below -20°C; it is sometimes termed the "defect" moment because its origin is postulated to be related to the effect of lattice defects on the anti-ferromagnetism (Jacobs and Bean, 1958). Recently, Smith and Fuller (1967) have detected a high-temperature moment, present over a range of 40-50°C above the Curie point of the spin-canted moment. They correlate this high-temperature moment with the low-temperature "defect" moment also present in their crystals, and conclude that a defect moment is present at all temperatures up to the "true" antiferromagnetic Neel point of 725°C.

Such a Neel point was first suggested by Aharoni et al. (1962) on the basis of two transitions (675 and 725°C) in differential thermal analysis curves of hematite. These temperatures were later found to be in error (Aharoni et al., 1963) and it was stated that only the higher transition (at about 690°C) was magnetically significant, but Smith and Fuller's results now apparently confirm the 725°C Neel point. If so, a further puzzling problem is posed: unless at 675°C, the spin sub-lattices again rotate out of the basal plane, as at the Morin transition, there is no convincing reason why the spin-canted moment should not be detectable between 675 and 725°C. Asymmetry in the basal plane anisotropy of the type suggested by Aharoni et al. (1962) could reduce the magnitude of the moment above 675°C by several times, but surely could not make it entirely unmeasurable when it is easily measurable only a few degrees below the Curie point.

Paleomagnetists are interested in hematite because the stable remanence of red sediments seems to be due to fine-grained hematite (Collinson, 1967). Previous studies of hematite have concentrated on coarse-grained material, frequently single crystals, but it is uncertain whether the measured data really apply to red beds in view of the strong grain size dependence of the properties of hematite reported by Chevallier and Mathieu (1943). In the present study therefore, fine-grained material in the single-domain range (0.2-0.7μ) was used. Since a prime objective was to attempt to detect a high-temperature moment, synthetic pure hematite was used to enhance measurement sensitivity, the hematite content of red sediments being commonly only a few percent (Collinson, 1968).

Magnetization (J-H) curves were measured at 16 temperatures between -196°C and 710°C in fields between -10 and +10 kOe. Some typical results are shown in Fig. 1. The room temperature results resemble the hysteresis curves reported by Collinson (1968) for red bed samples, and are in marked contrast to the curves usually found for coarse-grained hematites, in which the ferromagnetic component has a narrow range of coercivities below a few thousand oersteds. Curves measured in the spin-canting range (at 24, 170, 300, 400, 500, 580, 625, 660 and 670°C) showed a distinct and easily measured parasitic ferromagnetism, but with the exception of one curve measured near the Morin transition (at -28°C), which showed slight hysteresis, the low-temperature results (at -53, -83, -146 and -196°C) indicated pure antiferromagnetism. A single curve was measured at 710°C, above the Curie point of 679°C (confirmed by independent measurements with a Curie point meter) but below the supposed true Neel point of 725°C. It also was perfectly linear and showed no hysteresis. It is estimated that the defect moment in this sample, if present at all, must be less than 2% of the spin-canted moment.

Smith and Fuller's study of natural single crystals indicates that the spin-canted moment is relatively soft compared to the defect moment. obviously the same is not true for fine-grained hematite: the spin-canted moment of the present sample is very hard, being saturated in 10 kOe only above 500°C. To examine the complete spectrum of coercivities of the spin-canted moment at ordinary temperatures, the hysteresis curve in 30 kOe (shown in Fig. 1) was measured at 24°C. The precision was considerably less than that of the 10 kOe curves, but was sufficient to show that the room temperature coercivity spectrum extends up to 15 kOe at least.

The 30 kOe curve also enabled a separation to be made between the magnetization due to the antiferromagnetic susceptibility and that due to parasitic ferromagnetism at 24°C. In general agreement with previous studies (e.g. Neel and Pauthenet, 1952), the antiferromagnetic susceptibility was approximately constant, varying only 25% between 24 and 710°C, while the parasitic ferromagnetism (0.22 emu/g at 24°C) decreased very gradually with temperature, dropping off sharply only within 30° of the Curie point. At 670°C, only 10° below the Curie temperature, the spin-canted moment retained about 30% of its room temperature intensity. Despite this, there was no trace of any moment in the 710°C magnetization curve nor in a J_{sat} -T curve above 679°C.

The properties of hematite seem to be rather variable, and the measurements reported here do not rule out the possibility that defect moments play a role in the stable remanence of red sediments. However, the results do indicate that a high temperature moment is not always present above the Curie temperature. The lack of any trace of the spin-canted moment above

679°C sheds doubt on the existence of a Neel temperature different from the Curie temperature.

It can also be stated with certainty that the spin-canted moment is not soft in fine-grained hematite. In fact, the coercivity spectrum of the spin-canted moment is incompatible with present data on basal plane anisotropy (Banerjee, 1963; Flanders and Schuele, 1964; Anderson et al., 1954) which predict coercivities of several hundred oersteds at most. Of course, it is quite possible that the values of basal plane anisotropy determined from single crystal measurements are rather different from those of fine grains. In any case, whatever the origin of its high coercivity, the spin-canted moment must carry an important fraction of the stable remanence of fine-grained natural hematites.

This work was carried out at the Institute of Solid State Physics, University of Tokyo, by the kind permission of Prof. S. Chikazumi and Prof. Y. Ishikawa. I am very grateful to Dr. T. Mizoguchi for the use of his magnetic balance and for his constant help during the experiments.

References

Aharoni, A., E. H. Frei and M. Schieber (1962), Phys. Rev. 127, 439; (1963), ibid. 129, 2835.

Anderson, P. W., F. R. Merritt, J. P. Remeika and W. A. Yager (1954), ibid. 93, 717.

Banerjee, S. K. (1963), Phil. Mag. 8, 2119.

Chevallier, R. and S. Mathieu (1943), Annls. Phys. 18, 258.

Collinson, D. W. (1967), Geophys. J. Roy. Astr. Soc. 12, 197; (1968), Earth & Planetary Sci. Lett. 4, 417.

Dzialoshinskii, I. (1958), J. Phys. Chem. Solids 4, 241.

Flanders, P. J. and W. J. Schuele (1964), Phil. Mag. 9, 485.

Jacobs, I. S. and C. P. Bean (1958), J. Appl. Phys. 29, 537.

Lin, S. T. (1960), ibid. 31, 273S.

Moriya, T. (1960), Phys. Rev. 120, 91.

Neel, L. and R. Pauthenet (1952), C. R. Acad. Sci. (Paris) 234, 2172.

Smith, R. W. and M. Fuller (1967), Science 156, 1130.

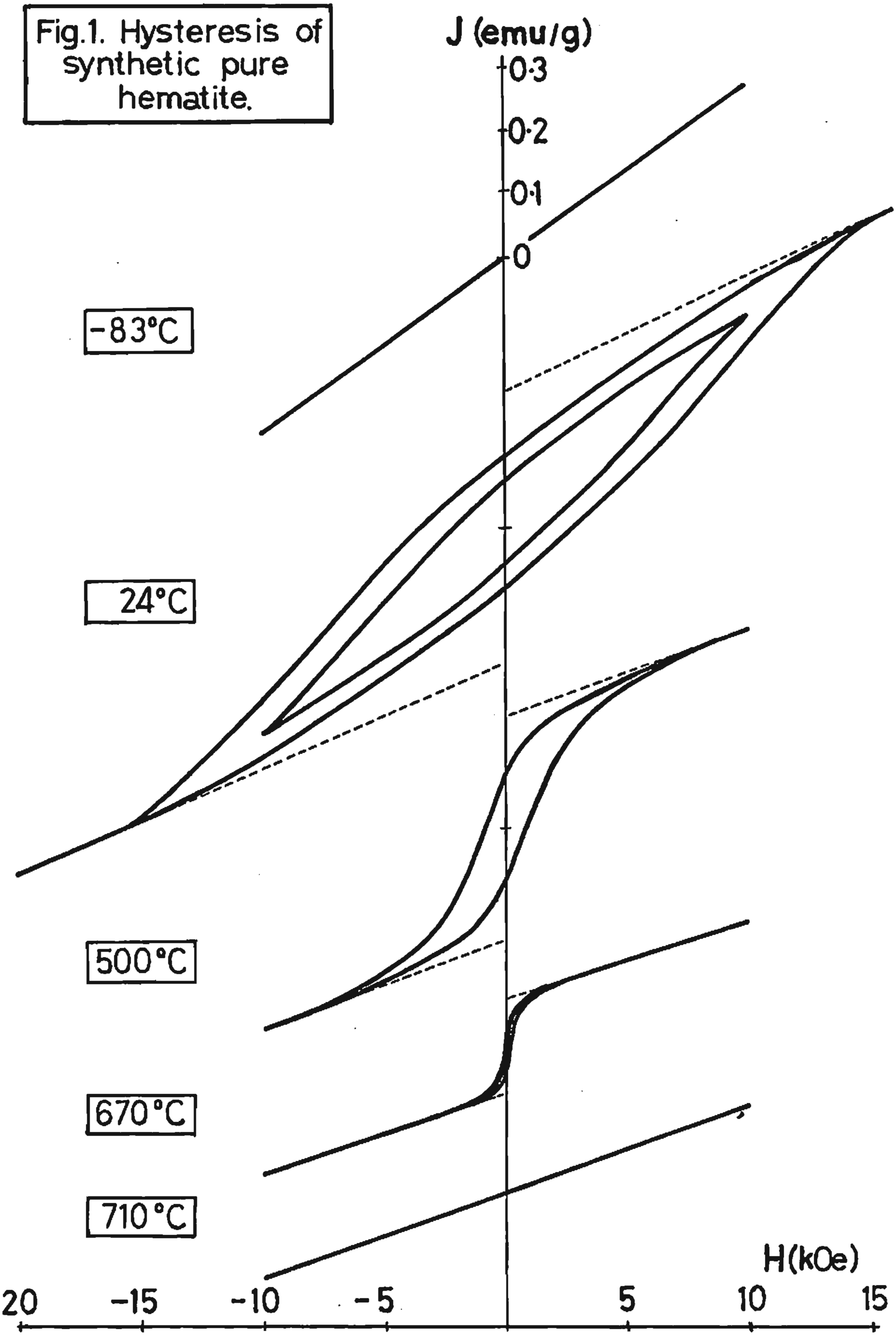

Dunlop Fig. 1 (of 1)

13. On the Unstable Natural Remanent Magnetization of Rocks as a Paleogeomagnetic "Fossil"*

Haruo Domen**

Faculty of Education, Yamaguchi University

753 Japan

Seventeen years ago the coexistence of both normal and reversed natural remanent magnetizations (nrm) was found in the early Pleistocene or late Pliocene basaltic lava flow at Kawajiri-misaki, Yamaguchi Prefecture, Southwest Japan (Asami & Domen, 1954). It was once understood that the reversed nrm was due to a reversed geomagnetic field at the time the lava flows erupted, and normal nrm was neglected because of its instability. However, the coexistence of both normal and reversed nrm, even in so small a portion of the lava flow, has remained a mystery. Was the earth's magnetic field reversed at that time or did self-reversal take place?

In this report, the author proposes a possible self-reversal mechanism as a solution to this mysterious phenomenon. He also considers that the unstable nrm might be usable in some cases as a paleogeomagnetic "fossil" rather than the stable nrm which usually seems to be good indicator of the earth's magnetic field in the past.

One half of the rock specimens coming from the lowest lava flow at Kawajiri-misaki showed normal nrm and the other half were reversed; even within a fist-sized specimen, the coexistence of both the polarities appeared.

** This will be read at 1969 Annual Meeting of A.G.U. at Washington, D.C., U.S.A. and details will appear in the Bulletin of Faculty of Education, Yamaguchi University, Vol. 18, Part II (March 1970).

** Now at Department of Earth Sciences, Washington University, St. Louis, Mo., U.S.A.

An nrm-intensity on the order of 10^{-2} emu/g was found in only about 10% of all of normal samples. 60% of the normal specimens showed orders of 10^{-3} emu/g and the rest, say 30%, were around 10^{-4} emu/g. On the other hand, about 70% of the reversely magnetized rock specimens had intensities on the order of 10^{-4} and the remainder were on the order of 10^{-3}.

The scattering of the nrm-directions of the normal specimens was much greater than that of the reversed specimens.

Thermo-magnetic analysis of the ferromagnetic rock-forming minerals showed that the Curie points of the normally magnetized specimens have three maximum-frequencies. The highest frequency among them falls into the medium temperature range, say roughly between 150°C and 450°C. However, the reversed specimens showed a frequency distribution with two maxima, one lower than 150°C and the other higher than 450°C.

This tendency is also recognized generally in other lava flows in the Kawajiri-misaki district, in which some lava flows show only normal nrm and others only reversed. That is to say, a lava flow in which only normal nrm has been found, shows the medium Curie-point with greatest frequency and a lava flow having only reversed nrm shows the lower and higher Curie-points.

When the normal specimens were heated up above their highest Curie-point in non-magnetic space, the nrm intensity decreased moderately with increasing temperature and vanished at the highest Curie temperature, but the reversed specimens showed a rather peculiar characteristic. That was the abrupt inversion of the nrm-direction to the normal direction in the medium temperature range; approximately between 150°C and 450°C. And as the temperature increased above this temperature range, the polarization switched to the original reversed direction again and finally vanished.

One half of the original nrm intensity of specimens with normal polarity was easily removed by an a.c. demagnetizing field whose peak value was 300 Oe. The same amount of the initial intensity of the reversed specimens remained after demagnetization in an a.c. field greater than 500 Oe.

The initial slope of the chemical demagnetization curve for specimens with normal polarity was somewhat steeper than that for reversed specimens. On the other hand, the tangent of the second stage of the demagnetization curve is steeper for the reversed nrm than for the normal.

The present experimental results strongly indicate the possible occurrence of exsolution. The reasoning is as follows:

1) The grain size of the ferromagnetic crystals would have been greatly reduced if exsolution had occurred, since exsolved titanomagnetites have volumes much smaller than 1 micron[8].
2) The reduced grains have higher coercive force than the unexsolved grains.
3) The domain wall movements which had occurred in a large unexsolved titanomagnetite were suppressed to a considerable degree by the existence of the exsolved phase in the titanomagnetite.

The reversely magnetized remanent might be due to the exsolved phases whose Curie-points are lower or higher than those of the original single-phased titanomagnetite, and the normal polarity resides in the titanomagnetite with the intermediate Curie-point. Thus, it could be the unexsolved single-phased titanomagnetite which bears the real fossil magnetization recording the earth's field in the geologic past. But this has been overshadowed by the opposed directions of the exsolved phases.

The present study draws the conclusion that the geomagnetic field at the time when the Kawajiri-misaki lava flows effused was normal in the direction parallel to the earth's present magnetic field. Although the radiometric dating is not completed yet, the age seems to be at the Pliocene-Pleistocene boundary from the geological or the geochemical view points.

Most investigators have paid no attention to such an unstable nrm, but the present author would like to propose that even unstable nrm might be used as a paleogeomagnetic "fossil" under such special conditions as exist in the Kawajiri-misaki basaltic lavas.

References

Asami, E. and H. Domen, (1954), On the natural remanent magnetization of basalts in northern sea-side district of Nagato and sedimentary rocks in Susa-Tertiary layer (in Japanese). Yamaguchi J. Sci. 5, 1-20.

14. Application of an Automatically Recording Method to the Astaticmagnetometer

Isao Muroi

Department of Earth Science, Science Education Institute of Osaka Prefecture

I. Introduction

The astaticmagnetometer used by means of a lamp-scale reading has been in some inconveniences.

It was tried to improve this reading to record automatically the intensity of magnetization of rock samples. For the purpose of detecting the deviation of the suspended mirror, two solar cells were employed. Out put from the cell is amplified and recorded. At the same time, the rotation angle of the sample stage was detected by using CdS (one of Photocell).

This new apparatus is tested for use and application. Some examples were shown.

II. Apparatus

1. Detecting the deviation of the suspended system

It is well-known that a silicon solar cell generates electric current corresponding to quantity of illumination. A basic idea is detecting the current from the astaticmagnetometer. For this purpose the rectangular surface of the cell is shaded to get a wedge shaped surface for the illumination as shown in Fig. 1. Consequently, as the illumination spot for the cell moves either to the right or left, the area of the surface to the spot changes and out put from the cell varies. In this case, two solar cells were connected differentially in its electric porality.

When the spot is just on the center of both cells, electric current is zero. But when the spot deviates, the effective surface area is changed. This is based on the fundamental principle that the deviation is converted to electric current, since the relation between the surface area and the electric power is linear. The two cells were fixed at the bottom of the black box which is set parallel to the suspended system of the magnetometer (Sokkisha Co.). The light is going through a tungusten lamp. The light from the mirror Mm which is fixed at the suspended system is reflected again on the surface of the glass plate G to the cells. The distance between the plate and the cell is 28 cm. The cell is a type of SPD-540 (Hayakawa Electric Co.) with the size of 10mm $\times$ 20mm and has maximum out put of about 12μA at a 900 mμlight length. A source of the light is 6 volt AC. The out put signal from the cell is amplified by a DC amplifier (AD-7, TOA Electronics Co.) and recorded by a recorder (EPR-10A, TOA Electronics Co.). Both of them are used at a 10 mV range. Lamp-scale is also used as a monitor. Chart speed is 20mm per minute. Fig. 2 indicates the circuit.

2. Detecting the rotation angle of the samples

Twelve mirrors Ms are fitted around the sample stage by 30 degrees. On the other hand, a source of light and a CdS are set up at a distance of 2 m from the stage. The CdS is connected to a relay which drives a marker pen. Rotating the stage, each mirror passes through a rest position and the reflected light from the mirror arrives to the CdS. The pulse pattern is appeared by the pen on the chart. The CdS is a type of 2PR-14 (Matsushita Electric Co.). A light source is 6 volt AC. Fig. 3 indicates the circuit.

Fig. 4 shows a schematic view of the arrangement of the automatically recording system.

III. Preliminary Test

By weak magnetic field produced by the sensitive coil, a correlation between the deflection of the suspended mirror and out put from the cell was examined. The result is shown in Fig. 5. The abscissa is the deflection on a lamp-scale and the angle in minute equal to the deflection. The ordinate shows the out put voltage from the cell. In this figure, the deflection of 1 cm (equivalent to 17' in this deflection angle) corresponds to the out put of 2 mV and 22 division on the chart at 10 mV range of the recorder. In other words, the deflection of 1' is equal to 118 micro volt and 1.3 division on the chart. The sensitivity of the magnetometer was $2.4 \times 10^{-6} (\frac{oe}{mm})$ on the lamp-scale, though the magnetometer has higher sensitivity.

IV. Application

Fig. 6 is a record of back ground noise at day and night in the laboratory. Very large difference of the noise between day and night were recognized. The most calm time is about from 1 to 4:30 a.m. This noise is probably affected by subway at a distance of 500 m from the laboratory.

Fig. 7 is an example of a rock sample, Shimakuma tuff of Osaka Group, Pleistocene sediment collected from Mino City, northern Osaka Prefecture. Each component of a specimen was measured twice in the opposite side. Hence a specimen with three components was measured six times in all. The size of the rock specimen is 5 cm $\times$ 5 cm $\times$ 5 cm. The intensity of this sample is $6.3 \times 10^{-6} (\frac{emu}{gr})$. The marks on the right side of this record are showing each angle of 30 degrees.

Fig. 8 is the case of Pink tuff of the same group mentioned above. The intensity of this remanence is $1.1 \times 10^{-5} (\frac{emu}{gr})$.

V. Discussion

The measurement was carried out at maximum deflection of 5 cm on the lamp-scale which corresponds to the deflection angle of $1^{\circ}26'$ and the deviation to the cell is 2.5 mm. It is not difficult to measure the intensity of magnetization of the order of 10^{-8} ($\frac{emu}{gr}$). Further, for a sample of marine mudstone of the same group, the intensity of 7.1×10^{-7} ($\frac{emu}{gr}$) was measured.

Though the effect depending on fluctuation of power source of light was not yet recognized, it is desirable to set a voltage stabilizer.

Some advantages of this method are as follows;

(1) Observations are carried out easier than that of lamp-scale reading.

(2) Since the value is recorded continuously, it is facile to examine whether the sample is suitable or not.

(3) As the sensitivity is higher, it is applicable to sedimentary rocks with very weak intensity of magnetization.

There are two points to improve for more convenient use; the one is to adopt a motor drive system of the sample stage and the other is to convert the analogous signal to the dizitalized one and to print the value by a printer in order to avoid trouble to read.

The author gratefully thanks Dr. I. Kato, the head of the Department of Earth Science, Science Education Institute of Osaka Prefecture and the other staff of the same Dept. for suggesting this method and advising technics throughout.

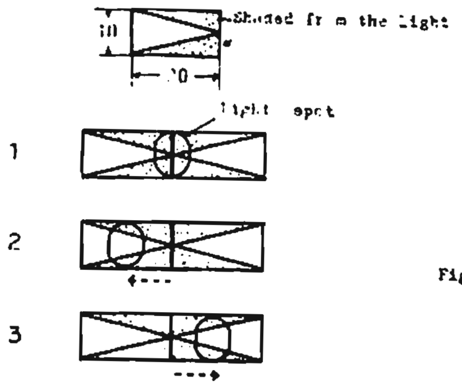

Fig.1 Solar Cell and light spot.

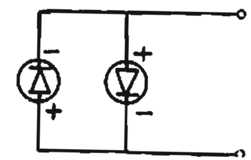

Fig.2 Two Cells connected with opposit porality.

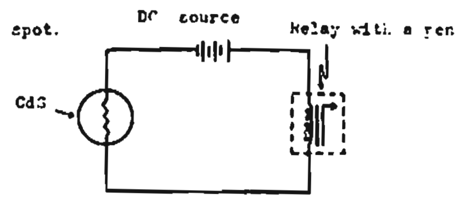

Fig.3 Circuit of the CdS and the relay

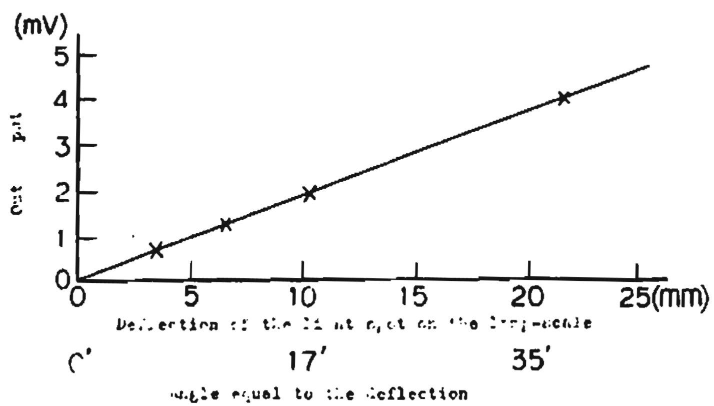

Fig. 5 Relation between the deflection and the out put.

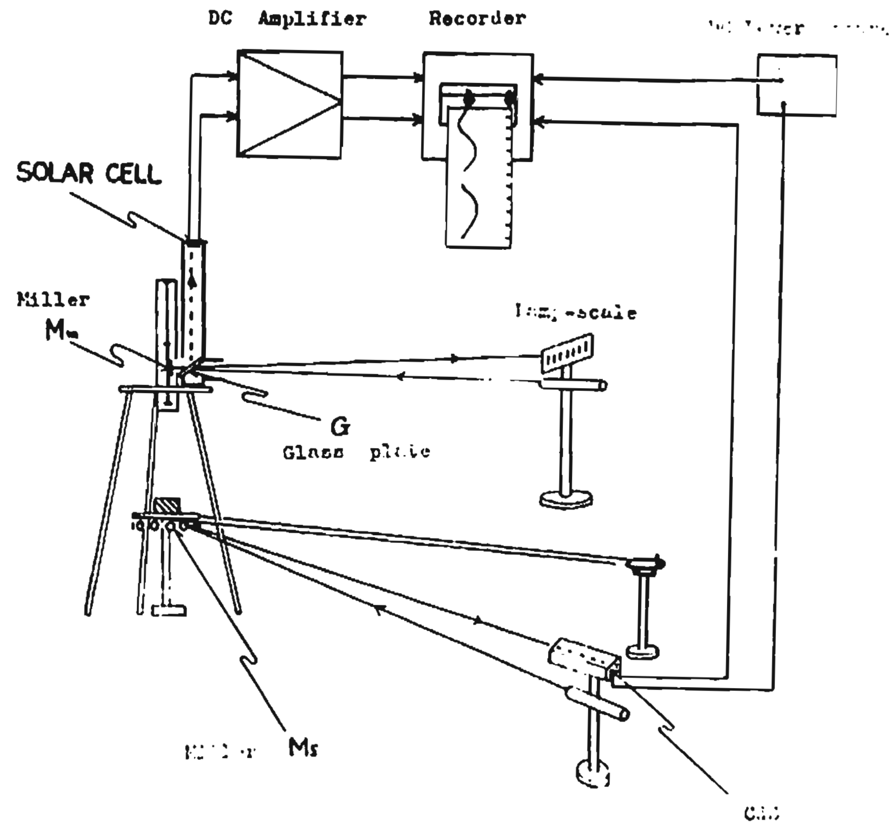

Fig. 4 Schematic view of the arrangement of the automatically recording system.

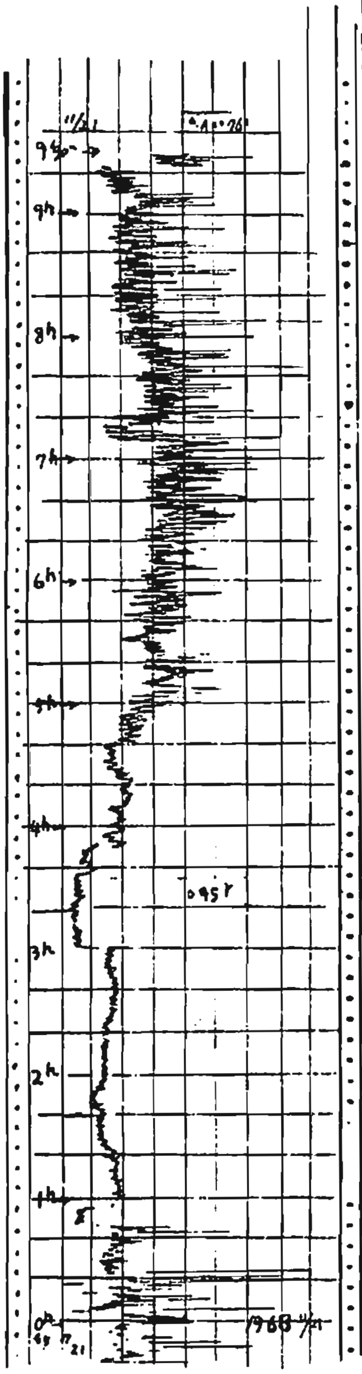

Fig. 6

Continuous record

at day bnd night

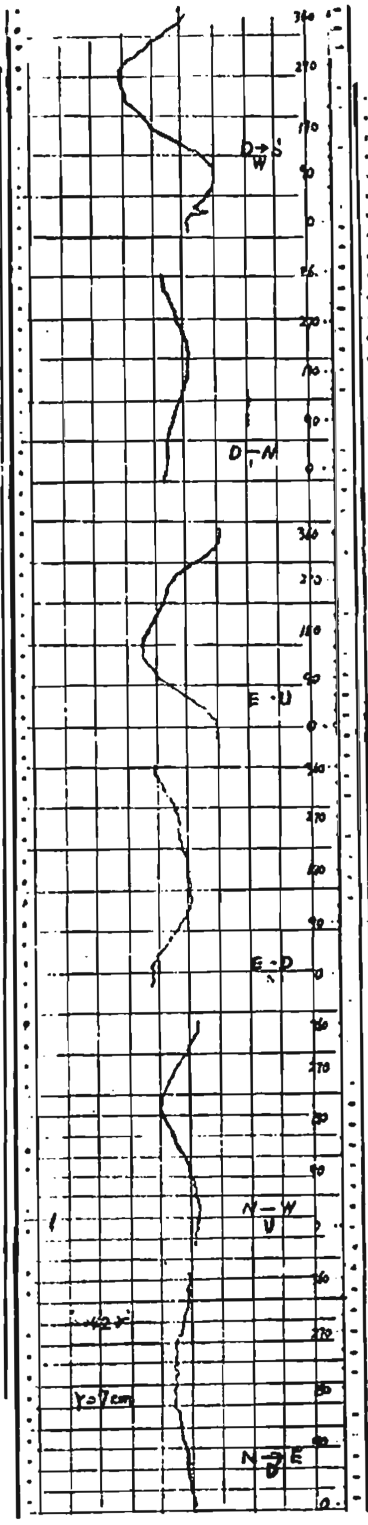

Fig. 7

Shimakuma tuff

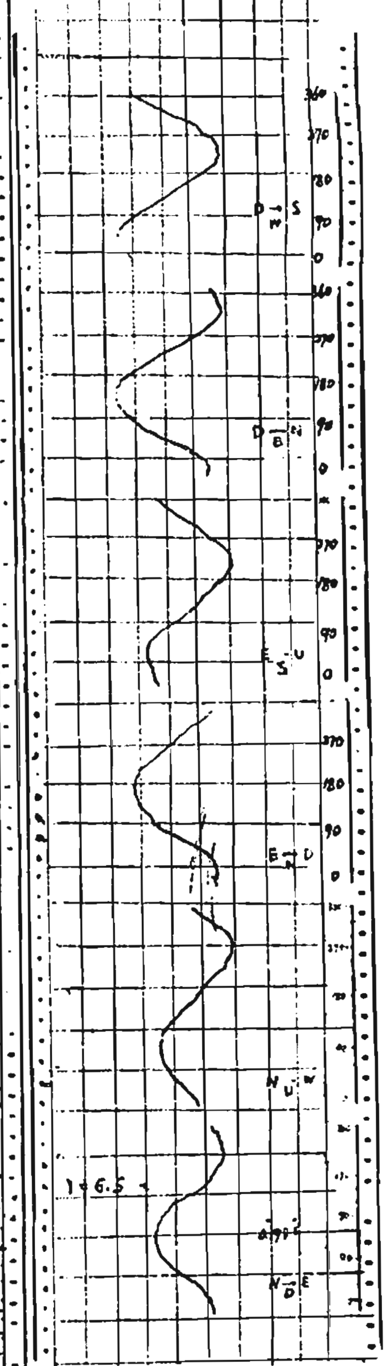

Fig. 8

Pink tuff